

The SUSY EW-like corrections to top pair production in photon-photon collisions

Zhou Mian-Lai^b, Ma Wen-Gan^{a,b,c}, Han Liang^b, Jiang Yi^b and Zhou Hong^b

^aCCAST (World Laboratory), P.O.Box 8730, Beijing 100080, China

^bModern Physics Department, University of Science and
Technology of China, Anhui 230027, China

^cInstitute of Theoretical Physics, Academia Sinica, P.O.Box 2735, Beijing 100080, China.

Abstract

We studied the one-loop contributions of the gaugino-Higgsino-sector to the process of top-pair production via $\gamma\gamma$ fusion at NLC in frame of the Minimal Supersymmetric Model(MSSM). We find that the corrections to $\gamma\gamma \rightarrow t\bar{t}$ and $e^+e^- \rightarrow \gamma\gamma \rightarrow t\bar{t}$ are found to be significant and can approach to a few percent and one percent, respectively. Furthermore, the dependences of the corrections on the supersymmetric parameters are also investigated. The corrections are not sensitive to $M_{SU(2)}$ (or $|\mu|$) when $M_{SU(2)} >> |\mu|$ (or $|\mu| >> M_{SU(2)}$) and are weakly dependent on the $\tan\beta$ with M_Q (or $|\mu|$) being large enough. But they are sensitive to the c.m.s. energy of the incoming photons.

PACS: 12.15.Lk, 12.60.Jv, 12.60.Cn, 12.60.Fr, 14.65.Ha

I. Introduction

The direct discovery of the top quark was presented in 1995 by the CDF and D0 experiments at the Fermilab Tevatron[1]. This is considered to be a remarkable success for the Standard Model(SM), since the present value of the top mass determined as PDG average is 173.8 ± 5.2 GeV from the direct observation of top events[2], which coincides with the indirect determination from the available precise data of electroweak experiments. But the SM has still some theoretical problems, like the hierarchy problem, the necessity of fine tuning and the non-occurrence of gauge coupling unification at high energies. The Supersymmetric Models(SUSY) can solve these problems by presenting an additional symmetry. Among all the extensions of the SM, the Minimal Supersymmetric Standard Model (MSSM)[3] is the most attractive one at present, since it is the simplest case of the SUSY models.

Due to the strong Yukawa couplings of top quark, the SUSY electroweak radiative corrections in top-pair production process are specially interesting. People believe that the accurate measurement of top quark pair production at the present and future colliders, should be effective in measuring the physical effects induced by the virtual supersymmetric particles and can afford us much information about the MSSM. Any deviation of the cross section of top-pair production from the SM predictions, including QCD and electroweak radiative corrections, would give a hint of new physics beyond the SM. Therefore testing this process to make the indirect search for virtual SUSY particles, is an attractive theme at present and future colliders.

In previous studies, many works were concentrated on the top-pair production at the e^+e^- and hadron colliders, such as the LEP2, LHC and Tevatron. In references[4], the SUSY QCD and SUSY electroweak-like (EW-like) corrections at pp colliders are presented. Recently, W. Hollik and C. Schappacher calculated the MSSM radiative one-loop corrections to top-pair production via e^+e^- collisions at LEP2 energies and found the relative difference between the predictions of the MSSM and the SM is typically below 10%[5].

The future Next Linear Collider(NLC) is designed to give the facilities for both e^+e^- and $\gamma\gamma$ collisions at the energy of $500 \sim 2000$ GeV with a luminosity of the order $10^{33} cm^{-2}s^{-1}$ [6]. A large number of top quark and other particle pairs can be produced at this machine operating in $\gamma\gamma$ collision mode with an agreeable production rate [7]. The events would be much cleaner than those produced at pp and $p\bar{p}$ colliders. It has been also found that the $t\bar{t}$ production rate in $\gamma\gamma$ collisions is

much larger than that from the direct $e^+e^- \rightarrow t\bar{t}$ production both with and without considering the threshold QCD effect of top quark pair at center-of-mass energies of the electron-positron system around 1 TeV[8]. Thus the process $\gamma\gamma \rightarrow t\bar{t}$ has a large potential for studying top physics directly.

The next-to-leading order QCD corrections in the SM and MSSM for this process both for polarized and unpolarized photon-photon collisions have been discussed in detail in Ref.[9]. There it was shown that the QCD corrections in both the SM QCD and the MSSM QCD are about 10% and of the order -10^{-2} , respectively. A. Denner, S. Dittmaier and M. Strobel calculated the corrections to the process $\gamma\gamma \rightarrow t\bar{t}$ in the electroweak standard model and found that the correction reduction for unpolarized or equally polarized photons can reach almost 10% close to threshold [10]. In the reference[11], C.S. Li et al. calculated the $O(\alpha m_t^2/m_W^2)$ Yukawa corrections from Higgs-sector to top pair production via photon-photon collision in the SM, the general two-Higgs-doublet model (2HDM) as well as the MSSM. They found that the correction to the cross section is about a few percent in the SM, but the correction can be more significant ($>10\%$) in the MSSM. Therefore the SUSY loop contributions have considerable effects. In this paper, we study the possible effects from the additional EW-like one-loop corrections through the virtual presence of charginos, neutralinos and squarks at the NLC. We provide explicit analytical expressions for the form factors which parametrize the one-loop corrections of $\gamma\gamma \rightarrow t\bar{t}$ subprocess, and present numerical results both for the subprocess and process $e^+e^- \rightarrow \gamma\gamma \rightarrow t\bar{t}$ at the NLC.

The paper is organized as follows: In Sec. II, the theory about the chargino/neutralino is introduced, and the relative Feynman rules used in the calculation are listed. In Sec. III, we discuss the tree-level and one-loop EW-like correction cross section, respectively, and give the explicit analytical formulae for them. In Sec. IV, the numerical results and discussions are described. Finally, we give a short summary. In the appendix, the form factors used in the cross section calculations are listed in detail.

II. Lagrangian and Feynman Rules

We denote the process of the top-pair production via $\gamma\gamma$ fusion as

$$\gamma(p_3)\gamma(p_4) \longrightarrow \bar{t}(p_1)t(p_2), \quad (2.1)$$

where $p_{1,2}$ and $p_{3,4}$ represent the four-momenta of the outgoing top quark pair and the incoming photons, respectively. In this work, we consider one-loop corrections of the gaugino-Higgsino-sector in the MSSM to this process. At the one-loop EW-like correction order, the vertex $\gamma t\bar{t}$ is modified by the virtual exchange of two charginos $\tilde{\chi}_{i=1,2}^\pm$ and four neutralinos $\tilde{\chi}_{i=1\sim 4}^0$, which are respectively combinations of charged gaugino and Higgsino (for charginos), and neutral gaugino, Higgsino, photino and zino (for neutralinos). The mass eigenstates $\tilde{\chi}_{1,2,3,4}^0$, $\tilde{\chi}_{1,2}^\pm$ for the charginos and neutralinos are respectively obtained by diagonalizing the mass matrices X and Y in four component representation.[3][12]. The chargino mass term in lagrangian has the form:

$$\mathcal{L}_m = -\frac{1}{2}(\psi^+ \ \psi^-) \begin{pmatrix} 0 & X^T \\ X & 0 \end{pmatrix} \begin{pmatrix} \psi^+ \\ \psi^- \end{pmatrix}, \quad (2.2)$$

with 2×2 X defined in reference[3]. The two masses of chargino $m_{\tilde{\chi}_{1,2}^\pm}$ extracted from the diagonal elements of matrix X are worked out as

$$M_\pm^2 = \frac{1}{2} \left\{ M_{SU(2)}^2 + \mu^2 + 2m_W^2 \pm \left[(M_{SU(2)}^2 - \mu^2)^2 + 4m_W^4 \cos^2 2\beta + 4m_W^2 (M_{SU(2)}^2 + \mu^2 + 2M_{SU(2)}\mu \sin 2\beta) \right]^{1/2} \right\}, \quad (2.3)$$

As to the neutralino sector, the mass term in lagrangian has the form as:

$$\mathcal{L}_m = -\frac{1}{2}(\psi^0)^T Y \psi^0 + h.c., \quad (2.4)$$

The definition of the 6×4 matrix Y can also be found in [3] [12].

Since we do not take the CP violation into account, so all the possible CP phases[12] are assumed to be zero. The physical masses of neutralinos are obtained by utilizing the transformation matrix N to diagonalize the 4×4 mass matrix Y. The detailed steps to work out N and the diagonal matrix Y_D are described in reference [12]. The above equations show that the chargino and neutralino masses are related to the MSSM parameters $M_{SU(2)}$, $M_{U(1)}$, μ and $\tan \beta$. In our work we adopt the assumption that the $SU(2) \times U(1)$ theory is embedded in grand unified theory (GUT), so we have the following relation:

$$M_{U(1)} = \frac{5s_W^2}{3c_W^2} M_{SU(2)}. \quad (2.5)$$

In the MSSM, each quark has two scalar partners called squarks: \tilde{q}_L and \tilde{q}_R . Without considering CP phases, the mass matrix of scalar quark takes the following form:[13]

$$-\mathcal{L}_m = \begin{pmatrix} \tilde{q}_L^* & \tilde{q}_R^* \end{pmatrix} \begin{pmatrix} m_{\tilde{q}_L}^2 & a_q m_q \\ a_q m_q & m_{\tilde{q}_R}^2 \end{pmatrix} \begin{pmatrix} \tilde{q}_L \\ \tilde{q}_R \end{pmatrix}, \quad (2.6)$$

The expressions of the masses for the squark current eigenstates are listed in Appendix A Eqs.(A.1) \sim (A.3). Then the masses of \tilde{q}_1 and \tilde{q}_2 read

$$(m_{\tilde{q}_1}^2, m_{\tilde{q}_2}^2) = \frac{1}{2} \{ m_{\tilde{q}_L}^2 + m_{\tilde{q}_R}^2 \mp [(m_{\tilde{q}_L}^2 - m_{\tilde{q}_R}^2)^2 + 4a_q^2 m_q^2]^{\frac{1}{2}} \}. \quad (2.7)$$

The Feynman rules for the couplings of $t - \tilde{b}_{L,R} - \tilde{\chi}_{1,2}^+$ and $t - \tilde{t}_{L,R} - \tilde{\chi}_{1,2,3,4}^0$ are presented in Ref.[3]. The squark mixing angles $\theta_{\tilde{b}}$, $\theta_{\tilde{b}}$ and phases $\phi_{\tilde{b}}$, $\phi_{\tilde{b}}$ enter in the couplings when the weak eigenstates \tilde{q}_L, \tilde{q}_R above are transformed into the mass eigenstates \tilde{q}_1, \tilde{q}_2 . In this paper we denote the vertices in squark mass eigenstate basis as

$$\bar{t} - \tilde{b}_i - \tilde{\chi}_j^+ : V_{t\tilde{b}_i\tilde{\chi}_j^+}^{(1)} P_L + V_{t\tilde{b}_i\tilde{\chi}_j^+}^{(2)} P_R, \quad (2.8.1)$$

$$t - \bar{\tilde{b}}_i - \tilde{\chi}_j^+ : -V_{t\tilde{b}_i\tilde{\chi}_j^+}^{(2)*} P_L - V_{t\tilde{b}_i\tilde{\chi}_j^+}^{(1)*} P_R, \quad (2.8.2)$$

$$\bar{t} - \tilde{t}_i - \tilde{\chi}_j^0 : V_{t\tilde{t}_i\tilde{\chi}_j^0}^{(1)} P_L + V_{t\tilde{t}_i\tilde{\chi}_j^0}^{(2)} P_R, \quad (2.8.3)$$

$$t - \bar{\tilde{t}}_i - \tilde{\chi}_j^0 : -V_{t\tilde{t}_i\tilde{\chi}_j^0}^{(2)*} P_L - V_{t\tilde{t}_i\tilde{\chi}_j^0}^{(1)*} P_R, \quad (2.8.4)$$

respectively, where $P_{L,R} = \frac{1}{2}(1 \mp \gamma_5)$ and the explicit expressions of the notations defined in Eqs.(2.8.1) \sim (2.8.4) are listed in Eqs.(A.4) \sim (A.11) in Appendix A.

For the Feynman rules of the Higgs-quark-quark, Higgs-squark-squark, Higgs-chargino-chargino and Z(γ)-chargino-chargino, one can refer to Ref.[3]. The couplings of $Higgs(B) - \tilde{\chi}_k^+ - \tilde{\chi}_k^+$ have a general form as

$$V_{B\tilde{\chi}_k^+\tilde{\chi}_k^+} = V_{B\tilde{\chi}_k^+\tilde{\chi}_k^+}^s + V_{B\tilde{\chi}_k^+\tilde{\chi}_k^+}^{ps} \gamma_5 \quad (B = h^0, H^0, A^0, G^0), \quad (2.9)$$

The notations defined above which appear in the form factors, are explicitly expressed in Eqs.(A.12) \sim (A.15) of Appendix A.

For Higgs-quark-quark and Higgs-squark-squark couplings, we denote

$$H^0 - t - t : V_{H^0tt} = \frac{-igm_t \sin \alpha}{2m_W \sin \beta}, \quad (2.10.1)$$

$$h^0 - t - t : \quad V_{h^0 tt} = \frac{-igm_t \cos \alpha}{2m_W \sin \beta}, \quad (2.10.2)$$

$$A^0 - t - t : \quad V_{A^0 tt} \gamma_5 = \frac{-gm_t \cot \beta}{2m_W} \gamma_5, \quad (2.10.3)$$

$$G^0 - t - t : \quad V_{G^0 tt} \gamma_5 = \frac{-gm_t}{2m_W} \gamma_5, \quad (2.10.4)$$

The couplings of $H^0(h^0) - \tilde{q}_i - \tilde{q}_i$ ($i = 1, 2, q = t, b$) are

$$\begin{aligned} V_{H^0 \tilde{t}_1 \tilde{t}_1} &= \frac{-igm_Z \cos(\alpha + \beta)}{\cos \theta_W} \left[\left(\frac{1}{2} - \frac{2}{3} \sin^2 \theta_W \right) \cos^2 \theta_{\tilde{t}} + \frac{2}{3} \sin^2 \theta_W \sin^2 \theta_{\tilde{t}} \right] \\ &\quad - \frac{igm_t^2 \sin \alpha}{m_W \sin \beta} + \frac{igm_t}{2m_W \sin \beta} (A_t \sin \alpha + \mu \cos \alpha) \sin \theta_{\tilde{t}} \cos \theta_{\tilde{t}}, \end{aligned} \quad (2.11.1)$$

$$\begin{aligned} V_{H^0 \tilde{t}_2 \tilde{t}_2} &= \frac{-igm_Z \cos(\alpha + \beta)}{\cos \theta_W} \left[\left(\frac{1}{2} - \frac{2}{3} \sin^2 \theta_W \right) \sin^2 \theta_{\tilde{t}} + \frac{2}{3} \sin^2 \theta_W \cos^2 \theta_{\tilde{t}} \right] \\ &\quad - \frac{igm_t^2 \sin \alpha}{m_W \sin \beta} - \frac{igm_t}{2m_W \sin \beta} (A_t \sin \alpha + \mu \cos \alpha) \sin \theta_{\tilde{t}} \cos \theta_{\tilde{t}}, \end{aligned} \quad (2.11.2)$$

$$\begin{aligned} V_{H^0 \tilde{b}_1 \tilde{b}_1} &= \frac{igm_Z \cos(\alpha + \beta)}{\cos \theta_W} \left[\left(\frac{1}{2} - \frac{1}{3} \sin^2 \theta_W \right) \cos^2 \theta_{\tilde{b}} + \frac{1}{3} \sin^2 \theta_W \sin^2 \theta_{\tilde{b}} \right] \\ &\quad - \frac{igm_b^2 \cos \alpha}{m_W \cos \beta} + \frac{igm_b}{2m_W \cos \beta} (A_b \cos \alpha + \mu \sin \alpha) \sin \theta_{\tilde{b}} \cos \theta_{\tilde{b}}, \end{aligned} \quad (2.11.3)$$

$$\begin{aligned} V_{H^0 \tilde{b}_2 \tilde{b}_2} &= \frac{igm_Z \cos(\alpha + \beta)}{\cos \theta_W} \left[\left(\frac{1}{2} - \frac{1}{3} \sin^2 \theta_W \right) \sin^2 \theta_{\tilde{b}} + \frac{1}{3} \sin^2 \theta_W \cos^2 \theta_{\tilde{b}} \right] \\ &\quad - \frac{igm_b^2 \cos \alpha}{m_W \cos \beta} - \frac{igm_b}{2m_W \cos \beta} (A_b \cos \alpha + \mu \sin \alpha) \sin \theta_{\tilde{b}} \cos \theta_{\tilde{b}}, \end{aligned} \quad (2.11.4)$$

$$\begin{aligned} V_{h^0 \tilde{t}_1 \tilde{t}_1} &= \frac{igm_Z \sin(\alpha + \beta)}{\cos \theta_W} \left[\left(\frac{1}{2} - \frac{2}{3} \sin^2 \theta_W \right) \cos^2 \theta_{\tilde{t}} + \frac{2}{3} \sin^2 \theta_W \sin^2 \theta_{\tilde{t}} \right] \\ &\quad - \frac{igm_t^2 \cos \alpha}{m_W \sin \beta} + \frac{igm_t}{2m_W \sin \beta} (A_t \cos \alpha - \mu \sin \alpha) \sin \theta_{\tilde{t}} \cos \theta_{\tilde{t}}, \end{aligned} \quad (2.11.5)$$

$$V_{h^0\tilde{t}_2\tilde{t}_2} = \frac{igm_Z \sin(\alpha + \beta)}{\cos \theta_W} \left[\left(\frac{1}{2} - \frac{2}{3} \sin^2 \theta_W \right) \sin^2 \theta_{\tilde{t}} + \frac{2}{3} \sin^2 \theta_W \cos^2 \theta_{\tilde{t}} \right] \\ - \frac{igm_t^2 \cos \alpha}{m_W \sin \beta} - \frac{igm_t}{2m_W \sin \beta} (A_t \cos \alpha - \mu \sin \alpha) \sin \theta_{\tilde{t}} \cos \theta_{\tilde{t}}, \quad (2.11.6)$$

$$V_{h^0\tilde{b}_1\tilde{b}_1} = \frac{-igm_Z \sin(\alpha + \beta)}{\cos \theta_W} \left[\left(\frac{1}{2} - \frac{1}{3} \sin^2 \theta_W \right) \cos^2 \theta_{\tilde{b}} + \frac{1}{3} \sin^2 \theta_W \sin^2 \theta_{\tilde{b}} \right] \\ + \frac{igm_b^2 \sin \alpha}{m_W \cos \beta} - \frac{igm_b}{2m_W \cos \beta} (A_b \sin \alpha - \mu \cos \alpha) \sin \theta_{\tilde{b}} \cos \theta_{\tilde{b}}, \quad (2.11.7)$$

$$V_{h^0\tilde{b}_2\tilde{b}_2} = \frac{-igm_Z \sin(\alpha + \beta)}{\cos \theta_W} \left[\left(\frac{1}{2} - \frac{1}{3} \sin^2 \theta_W \right) \sin^2 \theta_{\tilde{b}} + \frac{1}{3} \sin^2 \theta_W \cos^2 \theta_{\tilde{b}} \right] \\ + \frac{igm_b^2 \sin \alpha}{m_W \cos \beta} + \frac{igm_b}{2m_W \cos \beta} (A_b \sin \alpha - \mu \cos \alpha) \sin \theta_{\tilde{b}} \cos \theta_{\tilde{b}}, \quad (2.11.8)$$

respectively.

III. Calculations

In the calculation, we take the t'Hooft gauge and adopt the dimensional reduction (DR) scheme [19], which is commonly used in the calculations of the MSSM radiative corrections as it preserves supersymmetry at least at one-loop order, to eliminate the ultraviolet divergences in the virtual loop corrections. We choose the on-mass-shell (OMS) scheme [20] for doing renormalization.

3.1 The tree-level formulae and notations.

In the process of top-pair production via photon-photon collision, the Mandelstam variables \hat{s} , \hat{t} and \hat{u} are defined as $\hat{s} = (p_1 + p_2)^2$, $\hat{t} = (p_1 - p_3)^2$, $\hat{u} = (p_1 - p_4)^2$. The corresponding Lorentz invariant matrix element at the lowest order for the reaction $\gamma\gamma \rightarrow t\bar{t}$ is written as

$$\mathcal{M}_0 = \mathcal{M}_{\hat{t}} + \mathcal{M}_{\hat{u}}, \quad (3.1.1)$$

where

$$\mathcal{M}_{\hat{t}} = \left[\bar{u}(p_3)(-ie\gamma_\mu) \frac{i}{\hat{t} - m_t} (-ie\gamma_\nu)v(p_4)\epsilon^\mu(p1)\epsilon^\nu(p2) \right], \quad (3.1.2)$$

$$\mathcal{M}_{\hat{u}} = \left[\bar{u}(p_3)(-ie\gamma_\nu) \frac{i}{\hat{\mu} - m_t} (-ie\gamma_\mu)v(p_4)\epsilon^\nu(p2)\epsilon^\mu(p1) \right]. \quad (3.1.3)$$

The corresponding differential cross section is obtained by

$$\frac{d\hat{\sigma}_0(\hat{t}, \hat{s})}{d\hat{t}} = \frac{N_c}{16\pi^2 \hat{s}} \bar{\sum}_{spins} |\mathcal{M}_0|^2, \quad (3.1.4)$$

where the summation with a bar over head means to sum up the spins of final states and average the spins of initial photons. After integration over \hat{t} , the total Born cross section with unpolarized incoming photons is worked out as

$$\hat{\sigma}_0(\hat{s}) = \frac{32\pi\alpha^2}{27\hat{s}} \left[2\hat{\beta}(\hat{\beta}^2 - 2) + (3 - \hat{\beta}^4) \ln \frac{1 + \hat{\beta}}{1 - \hat{\beta}} \right]. \quad (3.1.5)$$

where the kinematic factor is defined as

$$\hat{\beta} = \sqrt{1 - 4m_t^2/\hat{s}}. \quad (3.1.6)$$

The total cross section including the leading one-loop corrections in the frame of the MSSM is

$$\hat{\sigma} = \hat{\sigma}_0 + \delta\hat{\sigma}^{1-loop}, \quad (3.1.7)$$

where $\delta\hat{\sigma}^{1-loop}$ represents the interference term between tree-level and one-loop correction amplitudes.

3.2 Self-energies.

The top quark wave function corrections δZ_{tt} 's are determined in terms of the one-particle irreducible two-point function $i\Gamma(p^2)$ for top quarks in the DR mass basis. It should be written as[22]:

$$\Gamma_{tt}(p^2) = (\not{p} - m_t) + [\not{p}P_L\Sigma_{tt}^L(p^2) + \not{p}P_R\Sigma_{tt}^R(p^2) + P_L\Sigma_{tt}^{S,L}(p^2) + P_R\Sigma_{tt}^{S,R}(p^2)]. \quad (3.2.1)$$

With the Feynman rules of the interactions of top-sbottom-chargino and top-stop-neutralino, the corresponding unrenormalized chargino self-energies read (see

Fig.1(f))

$$\begin{aligned} \Sigma_{tt}^{S,L}(p^2) = \frac{1}{16\pi^2} \sum_{j=1,2} & \left(\sum_{i=1,4} m_{\tilde{\chi}_i^0} V_{t\tilde{t}_j\tilde{\chi}_i^0}^{(1)} V_{t\tilde{t}_j\tilde{\chi}_i^0}^{(2)*} B_0[-p, m_{\tilde{\chi}_i^0}, m_{\tilde{t}_j}] \right. \\ & \left. + \sum_{i=1,2} m_{\tilde{\chi}_i^+} V_{t\tilde{b}_j\tilde{\chi}_i^+}^{(1)} V_{t\tilde{b}_j\tilde{\chi}_i^+}^{(2)*} B_0[-p, m_{\tilde{\chi}_i^+}, m_{\tilde{b}_j}] \right), \end{aligned} \quad (3.2.2)$$

$$\begin{aligned} \Sigma_{tt}^{S,R}(p^2) = \frac{1}{16\pi^2} \sum_{j=1,2} & \left(\sum_{i=1,4} m_{\tilde{\chi}_i^0} V_{t\tilde{t}_j\tilde{\chi}_i^0}^{(2)} V_{t\tilde{t}_j\tilde{\chi}_i^0}^{(1)*} B_0[-p, m_{\tilde{\chi}_i^0}, m_{\tilde{t}_j}] \right. \\ & \left. + \sum_{i=1,2} m_{\tilde{\chi}_i^+} V_{t\tilde{b}_j\tilde{\chi}_i^+}^{(2)} V_{t\tilde{b}_j\tilde{\chi}_i^+}^{(1)*} B_0[-p, m_{\tilde{\chi}_i^+}, m_{\tilde{b}_j}] \right), \end{aligned} \quad (3.2.3)$$

$$\Sigma_{tt}^L(p^2) = -\frac{1}{16\pi^2} \sum_{j=1,2} \left(\sum_{i=1,4} |V_{t\tilde{t}_j\tilde{\chi}_i^0}^{(2)}|^2 B_1[-p, m_{\tilde{\chi}_i^0}, m_{\tilde{t}_j}] + \sum_{i=1,2} |V_{t\tilde{b}_j\tilde{\chi}_i^+}^{(2)}|^2 B_1[-p, m_{\tilde{\chi}_i^+}, m_{\tilde{b}_j}] \right), \quad (3.2.4)$$

$$\Sigma_{tt}^R(p^2) = -\frac{1}{16\pi^2} \sum_{j=1,2} \left(\sum_{i=1,4} |V_{t\tilde{t}_j\tilde{\chi}_i^0}^{(1)}|^2 B_1[-p, m_{\tilde{\chi}_i^0}, m_{\tilde{t}_j}] + \sum_{i=1,2} |V_{t\tilde{b}_j\tilde{\chi}_i^+}^{(1)}|^2 B_1[-p, m_{\tilde{\chi}_i^+}, m_{\tilde{b}_j}] \right). \quad (3.2.5)$$

Imposing the on-shell renormalization conditions given in Ref.[20] [22], one can obtain the renormalization constants for the renormalized top quark self-energies as[9]:

$$\delta\Sigma_{tt}(p^2) = C_L \not{p} P_L + C_R \not{p} P_R - C_S^- P_L - C_S^+ P_R, \quad (3.2.6)$$

The $\gamma\gamma$ and γZ^0 self-energies with only quark and squark one-loops were presented in reference[23]. We can see that the self-energies of $\gamma\gamma$ and γZ^0 have no contribution to the relevant counterterms of the γtt vertex. The renormalization constant for the $\Gamma_{\gamma tt}^\mu$ vertex is written in the form of

$$\delta\Gamma_{\gamma tt}^\mu = -ie\gamma^\mu [C^L P_L + C^R P_R]. \quad (3.2.7)$$

where

$$\begin{aligned} C_L &= \frac{1}{2}(\delta Z_{tt}^L + \delta Z_{tt}^{L\dagger}), \\ C_R &= \frac{1}{2}(\delta Z_{tt}^R + \delta Z_{tt}^{R\dagger}), \\ C_S^- &= \frac{m_t}{2}(\delta Z_{tt}^L + \delta Z_{tt}^{R\dagger}) + \delta m_t, \\ C_S^+ &= \frac{m_t}{2}(\delta Z_{tt}^R + \delta Z_{tt}^{L\dagger}) + \delta m_t. \end{aligned} \quad (3.2.8)$$

$$\delta m_t = \frac{1}{2} \tilde{Re} \left[m_t \Sigma_{tt}^L(m_t^2) + m_t \Sigma_{tt}^R(m_t^2) + \Sigma_{tt}^{S,L}(m_t^2) + \Sigma_{tt}^{S,R}(m_t^2) \right], \quad (3.2.9)$$

$$\begin{aligned} \delta Z_{tt}^L &= -\tilde{Re} \Sigma_{tt}^L(m_t^2) - \frac{1}{m_t} \tilde{Re} \left[\Sigma_{tt}^{S,R}(m_t^2) - \Sigma_{tt}^{S,L}(m_t^2) \right] \\ &\quad - m_t \frac{\partial}{\partial p^2} \tilde{Re} \left\{ m_t \Sigma_{tt}^L(p^2) + m_t \Sigma_{tt}^R(p^2) \right. \\ &\quad \left. + \Sigma_{tt}^{S,L}(p^2) + \Sigma_{tt}^{S,R}(p^2) \right\} \Big|_{p^2=m_t^2}, \end{aligned} \quad (3.2.10)$$

$$\begin{aligned} \delta Z_{tt}^R &= -\tilde{Re} \Sigma_{tt}^R(m_t^2) - m_t \frac{\partial}{\partial p^2} \tilde{Re} \left\{ m_t \Sigma_{tt}^L(p^2) + m_t \Sigma_{tt}^R(p^2) \right. \\ &\quad \left. + \Sigma_{tt}^{S,L}(p^2) + \Sigma_{tt}^{S,R}(p^2) \right\} \Big|_{p^2=m_t^2}, \end{aligned} \quad (3.2.11)$$

where \tilde{Re} takes the real part of the loop integrals. It ensures reality of the renormalized lagrangian.

3.3 Renormalized one-loop corrections.

The renormalized one-loop matrix element involves the contributions from all the self-energy, vertex, box, triangle and quartic interaction one-loop diagrams and their relevant counterterms. The Feynman diagrams for the process (2.1) are depicted in Fig.1, where (a) is for the tree-level and (b) ~ (f) are EW-like one-loop diagrams contributing to the cross section in the frame of the MSSM. Specifically, Fig.1(b.1 ~ 4) are the vertex diagrams, Fig.1(c.1 ~ 3) are the box diagrams, Fig.1(d.1 ~ 2) are the quartic interactions, Fig.1(e.1 ~ 2) are the triangle sectors, and Fig.1(f) is the self-energy diagram. In below, we denote them by the upper indexes of v , b , q , tr and $self$, respectively. The relevant Feynman rules are shown in section II[3]. In the calculation, some of the s-channel Feynman diagrams involving quark loops with the exchanging of γ or Z^0 boson in Fig.1(e.2) can be neglected, as the consequence of Furry theorem. It is because that the Furry theorem forbids the production of the spin-one components of the Z^0 and γ , and the contribution from the spin-zero component of the Z^0 vector boson coupling with a pair of chargino is very small and neglectable. The calculation also shows the γ and Z^0 exchanging s-channel diagrams in Fig.1(d.2) and Fig.1(e.1) with a squark loop have no contribution to the cross

section, in which the contribution from each of the γ and Z^0 exchanging s-channel diagrams in Fig.1(e.1) is canceled out by the corresponding one with exchanging incoming photons. Including all the diagrams appearing in Fig.1, the renormalized matrix elements for $t\bar{t}$ pair production in $\gamma\gamma$ collision is written as

$$\begin{aligned}
\delta\mathcal{M}_{1-loop} &= \mathcal{M}^v + \mathcal{M}^b + \mathcal{M}^q + \mathcal{M}^{tr} + \mathcal{M}^{self} \\
&= \mathcal{M}^{v,\hat{t}} + \mathcal{M}^{v,\hat{u}} + \mathcal{M}^{b,\hat{t}} + \mathcal{M}^{b,\hat{u}} + \mathcal{M}^q + \mathcal{M}^{tr,\hat{t}} + \mathcal{M}^{tr,\hat{u}} + \mathcal{M}^{self,\hat{t}} + \mathcal{M}^{self,\hat{u}} \\
&= \epsilon^\mu(p_3)\epsilon^\nu(p_4)\bar{u}(p_1)\{f_1\gamma_\mu\gamma_\nu + f_2\gamma_\nu\gamma_\mu + f_3\gamma_\mu p_{1\nu} + f_4\gamma_\mu p_{2\nu} \\
&\quad + f_5\gamma_\nu p_{1\mu} + f_6\gamma_\nu p_{2\mu} + f_7p_{1\mu}p_{1\nu} + f_8p_{1\mu}p_{2\nu} + f_9p_{1\nu}p_{2\mu} \\
&\quad + f_{10}p_{2\mu}p_{2\nu} + f_{11}\not{p}_3\gamma_\mu\gamma_\nu + f_{12}\not{p}_3\gamma_\nu\gamma_\mu + f_{13}\not{p}_3\gamma_\mu p_{1\nu} + f_{14}\not{p}_3\gamma_\mu p_{2\nu} \\
&\quad + f_{15}\not{p}_3\gamma_\nu p_{1\mu} + f_{16}\not{p}_3\gamma_\nu p_{2\mu} + f_{17}\not{p}_3p_{1\mu}p_{1\nu} + f_{18}\not{p}_3p_{1\mu}p_{2\nu} \\
&\quad + f_{19}\not{p}_3p_{1\nu}p_{2\mu} + f_{20}\not{p}_3p_{2\mu}p_{2\nu} + f_{21}\gamma_5\epsilon_{\mu\nu\alpha\beta}p_1^\alpha p_3^\beta \\
&\quad + f_{22}\gamma_5\epsilon_{\mu\nu\alpha\beta}p_2^\alpha p_3^\beta\}v(p_2), \tag{3.3.1}
\end{aligned}$$

with form factors

$$f_i = f_i^v + f_i^b + f_i^q + f_i^{tr} + f_i^{self} \quad (i = 1 \sim 22), \tag{3.3.2}$$

Here we have divided each matrix element \mathcal{M}^v , \mathcal{M}^b , \mathcal{M}^{tr} and \mathcal{M}^{self} into t-channel and u-channel parts. For each of the corresponding form factor we have

$$f_i^k = f_i^{k,\hat{t}} + f_i^{k,\hat{u}}, \quad (k = v, b, tr, self, \quad i = 1 \sim 22), \tag{3.3.3}$$

The vertex, box and triangle diagrams with exchanging photons(i.e., u-channel) are not shown in Fig.1. The amplitude parts from the u-channel vertex, box and quartic interaction corrections can be obtained from the t-channel's by doing exchanges as below:

$$\mathcal{M}^{j,\hat{u}} = \mathcal{M}^{j,\hat{t}}(t \rightarrow u, p_3 \leftrightarrow p_4, \mu \leftrightarrow \nu), \quad (j = v, b, tr, s) \tag{3.3.4}$$

Then we list only the explicit t-channel form factors in Appendix B. Now we can obtain the one-loop corrections to the cross section from the chargino and neutralino sectors for this subprocess in unpolarized photon collisions.

$$\delta\hat{\sigma}^{1-loop}(\hat{s}) = \frac{N_c}{16\pi\hat{s}^2} \int_{\hat{t}^-}^{\hat{t}^+} d\hat{t} \, 2Re \sum_{spins} (\mathcal{M}_0^\dagger \cdot \delta\mathcal{M}_{1-loop}), \tag{3.3.5}$$

where $\hat{t}^\pm = (m_t^2 - \frac{1}{2}\hat{s}) \pm \frac{1}{2}\hat{s}\beta$. The cross section of the top-pair production via photon-photon fusion at the e^+e^- linear collider, can be obtained by folding the cross section of the subprocess $\hat{\sigma}(\gamma\gamma \rightarrow t\bar{t}$ with the photon luminosity[14, 15][14, 16].

IV. Numerical Results and Discussions

The SUSY EW-like corrections to top-pair production process are strongly related to the fundamental MSSM parameters through the electroweak couplings involving top-quark, squark and chargino (neutralino), i.e. $V_{t\tilde{b}\tilde{\chi}^+}$ and $V_{t\tilde{t}\tilde{\chi}^0}$ as expressed in Eqs.(2.8.1 ~ 4). For our numerical calculation of squark sector, we take M_Q , $\theta_{\tilde{t}}$ and $\theta_{\tilde{b}}$ as input parameters, and we set $\theta_{\tilde{b}} = 0$, and $\theta_{\tilde{t}}$ approaches $\frac{\pi}{4}$, so that the masses of top squark pair split remarkably, while the split of the sbottom masses is minimized. From the Eq.(2.7) and relevant expressions, we can see that the parameter M_Q is strongly related to the masses of top and bottom squarks, therefore it would affect the MSSM correction quantitatively in some regions of the parameter space.

As stated in Section II, the correction should also depend on the fundamental MSSM parameters $\tan\beta$, $M_{SU(2)}$ and μ through gaugino and higgsino couplings. Note that these parameters take parts in the EW-like corrections not only through the chargino and neutralino mass spectra, but also through the couplings including their transformation matrices U , V and N .

We take some of the general constants as: $m_t = 175$ GeV, $m_Z = 91.187$ GeV, $m_b = 4.5$ GeV, $\sin^2\theta_W = 0.2315$, and $\alpha = 1/128$. And we adopt the following set of input parameters by default, in case that the parameter is not set as the independent variable of the figure and no special declaration has been presented on them:

$$\begin{aligned} \sqrt{\hat{s}} &= 500 \text{ or } 1000 \text{ GeV}, & \tan\beta &= 4 \text{ or } 40, \\ M_Q &= M_{SU(2)} = \mu = 200 \text{ GeV}, \\ \theta_{\tilde{t}} &= 44.325^\circ, & \theta_{\tilde{b}} &= 0. \end{aligned} \quad (4.1)$$

We use the analytical formulae for the masses of the MSSM Higgs bosons (including two-loop leading-log corrections and squark mixing effects) given in reference [17][18].

$$m_{h^0,H^0}^2 = \frac{1}{2} \left[TrM^2 \mp \sqrt{(TrM^2)^2 - 4detM^2} \right], \quad (4.2.1)$$

where

$$TrM^2 = M_{11}^2 + M_{22}^2, \quad detM^2 = M_{11}^2 M_{22}^2 - (M_{12}^2)^2, \quad (4.2.2)$$

with

$$\begin{aligned}
M_{12}^2 &= 2v^2 \left[\sin\beta \cos\beta (\lambda_3 + \lambda_4) + \lambda_6 \cos^2\beta + \lambda_7 \sin^2\beta \right] - m_{A^0}^2 \sin\beta \cos\beta \\
M_{11}^2 &= 2v^2 \left[\lambda_1 \cos^2\beta + 2\lambda_6 \cos\beta \sin\beta + \lambda_5 \sin^2\beta \right] + m_{A^0}^2 \sin^2\beta \\
M_{22}^2 &= 2v^2 \left[\lambda_2 \sin^2\beta + 2\lambda_7 \cos\beta \sin\beta + \lambda_5 \cos^2\beta \right] + m_{A^0}^2 \cos^2\beta,
\end{aligned} \tag{4.2.3}$$

where $v = 174.1 \text{ GeV}$. The mixing angle α is determined by

$$\sin 2\alpha = \frac{2M_{12}^2}{\sqrt{(Tr M^2)^2 - 4 \det M^2}}, \tag{4.2.4}$$

One can find the explicit expressions of $\lambda_i (i = 1, \dots, 7)$ in reference[17]. In this work, we take $m_{A^0} = 150 \text{ GeV}$.

Our numerical results are presented in figures. In Fig.2(a) and Fig.2(b), the correction $\Delta\sigma$ and the relative correction $\delta = \frac{\Delta\sigma}{\sigma_0}$ of the process (2.1) depending on the c.m.s. energy $\sqrt{\hat{s}}$ are plotted, respectively. From our analyses, we expect that for the curves of $\tan\beta = 4$ in Fig.2(a) and Fig.2(b), there should be some spikes or turning points at $\sqrt{\hat{s}} \sim 2m_{\tilde{b}_1} = 403 \text{ GeV}$, $2m_{\tilde{b}_2} = 415 \text{ GeV}$, $2m_{\tilde{\chi}_2^+} = 546 \text{ GeV}$, and $2m_{\tilde{t}_2} = 628 \text{ GeV}$ due to the resonance effects. But we see in both figures that the first two resonance points merge each other in the curves of $\tan\beta = 4$ because they are too near. For $\tan\beta = 40$, there are only two obvious resonance points can be seen on the curve in figure 2(a) in the vicinities of $\sqrt{\hat{s}} \sim 2m_{\tilde{b}_1} \sim 2m_{\tilde{b}_2} \sim 410 \text{ GeV}$ and $\sqrt{\hat{s}} = 2m_{\tilde{\chi}_2^+} = 531 \text{ GeV}$. While only one obvious resonance peak can be seen on the curve of $\tan\beta = 40$ at $\sqrt{\hat{s}} = 2m_{\tilde{\chi}_2^+} = 531 \text{ GeV}$ in Fig.2(b).

In Fig.3 ~ 6 we depicted the dependences of the relative radiative correction on the fundamental supersymmetric input parameters M_Q , $M_{SU(2)}$ and $|\mu|$, respectively. In each figure we take four data sets for discussion: (1) $\tan\beta = 4$, $\sqrt{\hat{s}} = 500 \text{ GeV}$; (2) $\tan\beta = 40$, $\sqrt{\hat{s}} = 500 \text{ GeV}$; (3) $\tan\beta = 4$, $\sqrt{\hat{s}} = 1 \text{ TeV}$; (4) $\tan\beta = 40$, $\sqrt{\hat{s}} = 1 \text{ TeV}$. From Fig.3 one can see the absolute value of the relative correction becomes generally larger when $\sqrt{\hat{s}}$ goes higher. The same feature is also shown in Fig.2. Fig.3 present that the absolute value of the relative correction goes down to a smaller constant with M_Q increasing. Since M_Q is related to the masses of squarks $\tilde{t}_{1,2}$ and $\tilde{b}_{1,2}$ as stated in Eq.(2.7), it can be easily understood as the feature of the decoupling effect. We can conclude that the smaller M_Q is, the more significant the correction

can be. We can read from Fig.3 that the relative correction can reach -2% when M_Q is about 150 GeV , and for large M_Q with same $\sqrt{\hat{s}}$ the parameter $\tan\beta$ tends to make little difference on the relative correction. In Fig.4, the corrections as the function of $M_{SU(2)}$ are plotted with the four data sets. The grooves around 230 GeV on the two curves for $\sqrt{\hat{s}} = 500 \text{ GeV}$ and the small heaves in the vicinity of 450 GeV on the two curves of $\sqrt{\hat{s}} = 1 \text{ TeV}$, are all because of the resonance effect: $\sqrt{\hat{s}} \sim 2m_{\tilde{\chi}_2^+}$. When $M_{SU(2)}$ is large, all of the four curves become very plain because of the decoupling effect. In Fig.5, there are two peaks at the position about $\mu \sim 470 \text{ GeV}$ on the curves of $\sqrt{\hat{s}} = 1 \text{ TeV}$ due to the resonance effect, but the resonance effects around the region $\mu \sim 230 \text{ GeV}$ on the curves with $\sqrt{\hat{s}} = 500 \text{ GeV}$ are not clear. And we can see that the correction is no longer sensitive to $\tan\beta$ and μ when μ gets larger than 600 GeV . This is because the parameter $\tan\beta$ and μ are not only related to the masses of sparticles, but also involved in some vertices which are concerned in our calculation. Both Fig.4 and Fig.5 show that the higher the c.m.s. energy $\sqrt{\hat{s}}$ is, the larger the relative corrections to subprocess are.

Fig.6 shows the cross section of the parent process $e^+e^- \rightarrow \gamma\gamma \rightarrow t\bar{t}$ including one-loop EW-like corrections as the function of c.m.s energy of incoming electron-positron pair. In Fig.7, the relative corrections for $\tan\beta = 4$ and $\tan\beta = 40$ are plotted, respectively. It is clear that the absolute value of the relative correction becomes larger with the increasing of the e^+e^- c.m.s energy. The reduction of the cross section of the parent process due to the one-loop EW-like correction can approach to one percent.

V.Summary

In this work we have studied the complete one-loop radiative corrections from the gaugino-Higgsino-sector in the process $\gamma\gamma \rightarrow t\bar{t}$ in the frame of the MSSM at the NLC. This process has great importance at the future NLC operating in photon-photon collision mode. From the numerical calculation with several typical sets of input parameters, we find that the EW-like corrections from the chargino/neutralino sector can be a few percent for subprocess and can approach to one percent for the parent process. These corrections are smaller than the QCD corrections, but are comparable to the electroweak correction part from the Higgs sector in the MSSM. Therefore the correction from chargino/neutralino sector is also significant and un-

neglectable. We investigated also the dependences of the corrections on the supersymmetric parameters. With the variation of the parameters M_Q , $M_{SU(2)}$ and $|\mu|$, we can see some physical features, such as the decoupling effects, threshold effects and the resonance effects, where the relative correction can be significantly enhanced or diminished. We conclude that the EW-like one-loop correction to Born cross section is strongly dependent on the c.m.s. energy and the related MSSM parameters in some cases. We find that the correction is not sensitive to $M_{SU(2)}$ (or $|\mu|$) when $M_{SU(2)} \gg |\mu|$ (or $|\mu| \gg M_{SU(2)}$). The correction is weakly dependent on the ratio of the vacuum expectation values $\tan \beta$, when M_Q (or $|\mu|$) is large enough. But it is related to the c.m. energy of the incoming photons obviously.

Acknowledgement: These work was supported in part by the National Natural Science Foundation of China(project numbers: 19675033, 19875049) and the Youth Science Foundation of the University of Science and Technology of China.

Appendix

A. Some expressions defined in Lagrangian.

In the lagrangian shown in eq.(2.6), we denote \tilde{q}_L and \tilde{q}_R as the current eigenstates. For the up-type scalar quarks, we have

$$\begin{aligned} m_{\tilde{q}_L}^2 &= \tilde{M}_Q^2 + m_q^2 + m_Z^2 \left(\frac{1}{2} - Q_q s_W^2 \right) \cos 2\beta, \\ m_{\tilde{q}_R}^2 &= \tilde{M}_U^2 + m_q^2 + Q_q m_Z^2 s_W^2 \cos 2\beta, \\ a_q &= \mu \cot \beta + A_q \tilde{M}. \end{aligned} \tag{A.1}$$

For the down-type scalar quarks,

$$\begin{aligned} m_{\tilde{q}_L}^2 &= \tilde{M}_Q^2 + m_q^2 - m_Z^2 \left(\frac{1}{2} + Q_q s_W^2 \right) \cos 2\beta, \\ m_{\tilde{q}_R}^2 &= \tilde{M}_D^2 + m_q^2 + Q_q m_Z^2 s_W^2 \cos 2\beta, \\ a_q &= \mu \tan \beta + A_q \tilde{M}, \end{aligned} \tag{A.2}$$

where $Q_q = \frac{2}{3}$ (for up-type), $-\frac{1}{3}$ (for down-type) is the charge of the scalar quark, \tilde{M}_Q^2 , \tilde{M}_U^2 and \tilde{M}_D^2 are the self-supersymmetry-breaking mass terms for the left-handed and right-handed scalar quarks, and $s_W = \sin \theta_W$, $c_W = \cos \theta_W$. As an assumption at Planck scale, We choose $\tilde{M}_Q = \tilde{M}_U = \tilde{M}_D = \tilde{M}$. Since CP effects are not considered, the value a_q is real. When \tilde{q}_L and \tilde{q}_R are mixed, they give the mass eigenstates \tilde{q}_1 and \tilde{q}_2 . The mass eigenstates \tilde{q}_1 and \tilde{q}_2 are expressed in terms of the current eigenstates \tilde{q}_L , \tilde{q}_R as read

$$\tilde{q}_1 = \tilde{q}_L \cos \theta_q - \tilde{q}_R \sin \theta_q,$$

$$\tilde{q}_2 = \tilde{q}_L \sin \theta_q + \tilde{q}_R \cos \theta_q,$$

with

$$\tan 2\theta_q = \frac{2a_q m_q}{m_{\tilde{q}_L}^2 - m_{\tilde{q}_R}^2}. \quad (A.3)$$

The explicit expressions for the notations used in Eqs.(2.8.1) \sim (2.8.4) are listed as below

$$V_{t\tilde{b}_1\tilde{\chi}_j^+}^{(1)} = \frac{igm_t}{\sqrt{2}m_W \sin \beta} V_{j2}^* \cos \theta_{\tilde{b}}, \quad (A.4)$$

$$V_{t\tilde{b}_1\tilde{\chi}_j^+}^{(2)} = -ig(U_{j1} \cos \theta_{\tilde{b}} + \frac{m_b}{\sqrt{2}m_W \cos \beta} U_{j2} \sin \theta_{\tilde{b}}), \quad (A.5)$$

$$V_{t\tilde{b}_2\tilde{\chi}_j^+}^{(1)} = \frac{igm_t}{\sqrt{2}m_W \sin \beta} V_{j2}^* \sin \theta_{\tilde{b}}, \quad (A.6)$$

$$V_{t\tilde{b}_2\tilde{\chi}_j^+}^{(2)} = -ig(U_{j1} \sin \theta_{\tilde{b}} - \frac{m_b}{\sqrt{2}m_W \cos \beta} U_{j2} \cos \theta_{\tilde{b}}), \quad (A.7)$$

$$V_{t\tilde{t}_1\tilde{\chi}_j^0}^{(1)} = -ig\sqrt{2}(\frac{m_t}{2m_W \sin \beta} N_{j4}^* \cos \theta_{\tilde{t}} + \frac{2}{3} \tan \theta_W N_{j1}^* \sin \theta_{\tilde{t}}), \quad (A.8)$$

$$V_{t\tilde{t}_1\tilde{\chi}_j^0}^{(2)} = -ig\sqrt{2}((\frac{1}{6} \tan \theta_W N_{j1} + \frac{1}{2} N_{j2}) \cos \theta_{\tilde{t}} - \frac{m_t}{2m_W \sin \beta} N_{j4} \sin \theta_{\tilde{t}}), \quad (A.9)$$

$$V_{t\tilde{t}_2\tilde{\chi}_j^0}^{(1)} = -ig\sqrt{2}(\frac{m_t}{2m_W \sin \beta} N_{j4}^* \sin \theta_{\tilde{t}} - \frac{2}{3} \tan \theta_W N_{j1}^* \cos \theta_{\tilde{t}}), \quad (A.10)$$

$$V_{t\tilde{t}_2\tilde{\chi}_j^0}^{(2)} = -ig\sqrt{2}((\frac{1}{6} \tan \theta_W N_{j1} + \frac{1}{2} N_{j2}) \sin \theta_{\tilde{t}} + \frac{m_t}{2m_W \sin \beta} N_{j4} \cos \theta_{\tilde{t}}), \quad (A.11)$$

The shorted notations defined in Eq.(2.9), are explicitly expressed below.

$$V_{H^0\tilde{\chi}_k^+\tilde{\chi}_k^+}^s = \frac{-ig}{\sqrt{2}} [\cos \alpha Re(V_{k,1}U_{k,2}) + \sin \alpha Re(V_{k,2}U_{k,1})] \quad (A.12)$$

$$V_{h^0\tilde{\chi}_k^+\tilde{\chi}_k^+}^s = \frac{ig}{\sqrt{2}} [\sin \alpha Re(V_{k,1}U_{k,2}) - \cos \alpha Re(V_{k,2}U_{k,1})] \quad (A.13)$$

$$V_{A^0\tilde{\chi}_k^+\tilde{\chi}_k^+}^{ps} = \frac{g}{\sqrt{2}} [\sin \beta Re(V_{k,1}U_{k,2}) + \cos \beta Re(V_{k,2}U_{k,1})] \quad (A.14)$$

$$V_{G^0\tilde{\chi}_k^+\tilde{\chi}_k^+}^{ps} = \frac{-g}{\sqrt{2}} [\cos \beta Re(V_{k,1}U_{k,2}) - \sin \beta Re(V_{k,2}U_{k,1})] \quad (A.15)$$

B. Form Factors. In this appendix we list all the form factors for the one-loop correction diagrams by using some abbreviations for following expressions.

$$\begin{aligned} \bar{B}_0^{1,k} &= B_0[-p_1 - p_2, m_{\tilde{b}_k}, m_{\tilde{b}_k}] - \Delta, & \bar{B}_0^{2,k} &= \bar{B}_0^{1,k}(m_{\tilde{b}_k} \rightarrow m_{\tilde{t}_k}), \\ \bar{B}_0^{3,i,j} &= B_0[p_3 - p_1, m_{\tilde{\chi}_i^0}, m_{\tilde{t}_j}] - \Delta, & \bar{B}_1^{3,i,j} &= B_0[p_3 - p_1, m_{\tilde{\chi}_i^0}, m_{\tilde{t}_j}] + \frac{\Delta}{2}, \\ \bar{B}_0^{4,i,j} &= B_0[p_3 - p_1, m_{\tilde{\chi}_i^+}, m_{\tilde{b}_j}] - \Delta, & \bar{B}_1^{4,i,j} &= B_0[p_3 - p_1, m_{\tilde{\chi}_i^+}, m_{\tilde{b}_j}] + \frac{\Delta}{2}, \\ C_0^{1,i,j}, C_{ab}^{1,i,j} &= C_0, C_{ab}[-p_1, p_1 + p_2, m_{\tilde{\chi}_i^+}, m_{\tilde{b}_j}, m_{\tilde{b}_j}], \\ C_0^{2,i,j}, C_{ab}^{2,i,j} &= C_0, C_{ab}[-p_1, p_1 + p_2, m_{\tilde{\chi}_i^0}, m_{\tilde{t}_j}, m_{\tilde{t}_j}], \\ C_0^{3,k}, C_{ab}^{3,k} &= C_0, C_{ab}[-p_3, p_1 + p_2, m_{\tilde{\chi}_k^+}, m_{\tilde{\chi}_k^+}, m_{\tilde{\chi}_k^+}], \\ C_0^{4,k}, C_{ab}^{4,k} &= C_0, C_{ab}[p_3, -p_1 - p_2, m_{\tilde{b}_k}, m_{\tilde{b}_k}, m_{\tilde{b}_k}], \\ C_0^{5,k}, C_{ab}^{5,k} &= C_0, C_{ab}[p_3, -p_1 - p_2, m_{\tilde{t}_k}, m_{\tilde{t}_k}, m_{\tilde{t}_k}], \\ C_0^{6,i,j}, C_{ab}^{6,i,j}(k_1, k_2) &= C_0, C_{ab}[-k_1, k_1 + k_2, m_{\tilde{b}_j}, m_{\tilde{\chi}_i^+}, m_{\tilde{\chi}_i^+}], \\ C_0^{7,i,j}, C_{ab}^{7,i,j}(k_1, k_2) &= C_0, C_{ab}[-k_1, k_1 + k_2, m_{\tilde{\chi}_i^+}, m_{\tilde{b}_j}, m_{\tilde{b}_j}], \\ C_0^{8,i,j}, C_{ab}^{8,i,j}(k_1, k_2) &= C_0, C_{ab}[-k_1, k_1 + k_2, m_{\tilde{\chi}_i^0}, m_{\tilde{t}_j}, m_{\tilde{t}_j}], \\ D_0^{1,i,j}, D_{ab}^{1,i,j}, D_{abc}^{1,i,j} &= D_0, D_{ab}, D_{abc}[p_1, -p_3, -p_4, m_{\tilde{b}_j}, m_{\tilde{\chi}_i^+}, m_{\tilde{\chi}_i^+}, m_{\tilde{\chi}_i^+}] \end{aligned}$$

$$\begin{aligned}
D_0^{2,i,j}, D_{ab}^{2,i,j}, D_{abc}^{2,i,j} &= D_0, D_{ab}, D_{abc}[-p_1, p_3, p_4, m_{\tilde{\chi}_i^+}, m_{\tilde{b}_j}, m_{\tilde{b}_j}, m_{\tilde{b}_j}] \\
D_0^{3,i,j}, D_{ab}^{3,i,j}, D_{abc}^{3,i,j} &= D_0, D_{ab}, D_{abc}[-p_1, p_3, p_4, m_{\tilde{\chi}_i^0}, m_{\tilde{t}_j}, m_{\tilde{t}_j}, m_{\tilde{t}_j}] \\
D_0^{4,i,j}, D_{ab}^{4,i,j}, D_{abc}^{4,i,j} &= D_0, D_{ab}, D_{abc}[-p_3, p_1, -p_4, m_{\tilde{b}_j}, m_{\tilde{b}_j}, m_{\tilde{\chi}_i^+}, m_{\tilde{\chi}_i^+}]
\end{aligned}$$

$$A_t = \frac{i}{\hat{t} - m_t^2}, \quad A_u = \frac{i}{\hat{u} - m_t^2},$$

$$A_h = \frac{i}{\hat{s} - m_h^2}, \quad A_H = \frac{i}{\hat{s} - m_H^2}.$$

$$A_A = \frac{i}{\hat{s} - m_A^2}, \quad A_G = \frac{i}{\hat{s} - m_Z^2}.$$

$$F_1^{t\tilde{b}_j\tilde{\chi}_i^+} = -|V_{t\tilde{b}_j\tilde{\chi}_i^+}^{(1)}|^2 - |V_{t\tilde{b}_j\tilde{\chi}_i^+}^{(2)}|^2, \quad F_2^{t\tilde{b}_j\tilde{\chi}_i^+} = -V_{t\tilde{b}_j\tilde{\chi}_i^+}^{(1)*} V_{t\tilde{b}_j\tilde{\chi}_i^+}^{(2)} - V_{t\tilde{b}_j\tilde{\chi}_i^+}^{(2)*} V_{t\tilde{b}_j\tilde{\chi}_i^+}^{(1)},$$

and

$$G_1^{t\tilde{t}_j\tilde{\chi}_i^0} = -|V_{t\tilde{t}_j\tilde{\chi}_i^0}^{(1)}|^2 - |V_{t\tilde{t}_j\tilde{\chi}_i^0}^{(2)}|^2, \quad G_2^{t\tilde{t}_j\tilde{\chi}_i^0} = -V_{t\tilde{t}_j\tilde{\chi}_i^0}^{(1)*} V_{t\tilde{t}_j\tilde{\chi}_i^0}^{(2)} - V_{t\tilde{t}_j\tilde{\chi}_i^0}^{(2)*} V_{t\tilde{t}_j\tilde{\chi}_i^0}^{(1)}.$$

The one-particle-irreducible(1PI) correction to the vertex γtt stemming from squark, chargino and neutralino can be written in terms of form factors

$$\begin{aligned}
\Delta\Gamma_{\gamma tt}^\mu(k_1, k_2) &= g_1(k_1, k_2)k_1^\mu\gamma_5\cancel{k}_1 + g_2(k_1, k_2)k_2^\mu\gamma_5\cancel{k}_1 + g_3(k_1, k_2)k_1^\mu\gamma_5\cancel{k}_2 \\
&+ g_4(k_1, k_2)k_2^\mu\gamma_5\cancel{k}_2 + g_5(k_1, k_2)k_1^\mu\gamma_5 + g_6(k_1, k_2)k_2^\mu\gamma_5 \\
&+ g_7(k_1, k_2)\gamma_5\gamma^\mu\cancel{k}_1\cancel{k}_2 + g_8(k_1, k_2)\gamma_5\gamma^\mu\cancel{k}_1 + g_9(k_1, k_2)\gamma_5\gamma^\mu\cancel{k}_2 \\
&+ g_{10}(k_1, k_2)\gamma_5\gamma^\mu + g_{11}(k_1, k_2)k_1^\mu\cancel{k}_1 + g_{12}(k_1, k_2)k_2^\mu\cancel{k}_1 \\
&+ g_{13}(k_1, k_2)k_1^\mu\cancel{k}_2 + g_{14}(k_1, k_2)k_2^\mu\cancel{k}_2 + g_{15}(k_1, k_2)k_1^\mu \\
&+ g_{16}(k_1, k_2)k_2^\mu + g_{17}(k_1, k_2)\gamma^\mu\cancel{k}_1\cancel{k}_2 + g_{18}(k_1, k_2)\gamma^\mu\cancel{k}_1 \\
&+ g_{19}(k_1, k_2)\gamma^\mu\cancel{k}_2 + g_{20}(k_1, k_2)\gamma^\mu,
\end{aligned}$$

where k_1 and k_2 are the four-momenta of the lightest top quark pair and along their outgoing directions, respectively. In the equation above, the form factors of the Lorentz invariant structures including γ_5 do not contribute to the cross sections

of our subprocess. Therefore we shall list only the explicit expressions of the form factors g_i ($i = 11 \sim 20$). The form factors g_i ($i = 11 \sim 20$) are expressed as follows.

$$\begin{aligned}
g_{11}(k_1, k_2) &= \frac{ie}{16\pi^2} \sum_{i=1,2} \sum_{j=1,2} F_1^{t\tilde{b}_j \tilde{\chi}_i^+} (C_{11}^{6,i,j} - C_{12}^{6,i,j} + C_{21}^{6,i,j} + C_{22}^{6,i,j} - 2C_{23}^{6,i,j})(k_1, k_2) \\
&- \frac{ie}{32\pi^2} Q_b \sum_{i=1,2} \sum_{j=1,2} F_1^{t\tilde{b}_j \tilde{\chi}_i^+} (C_{11}^{7,i,j} - C_{12}^{7,i,j} + 2C_{21}^{7,i,j} + 2C_{22}^{7,i,j} - 4C_{23}^{7,i,j})(k_1, k_2) \\
&- \frac{ie}{32\pi^2} Q_t \sum_{i=1,4} \sum_{j=1,2} G_1^{t\tilde{t}_j \tilde{\chi}_i^0} (C_{11}^{8,i,j} - C_{12}^{8,i,j} + 2C_{21}^{8,i,j} + 2C_{22}^{8,i,j} - 4C_{23}^{8,i,j})(k_1, k_2) \\
\\
g_{12}(k_1, k_2) &= \frac{ie}{16\pi^2} \sum_{i=1,2} \sum_{j=1,2} F_1^{t\tilde{b}_j \tilde{\chi}_i^+} (C_{22}^{6,i,j} - C_{23}^{6,i,j})(k_1, k_2) \\
&+ \frac{ie}{32\pi^2} Q_b \sum_{i=1,2} \sum_{j=1,2} F_1^{t\tilde{b}_j \tilde{\chi}_i^+} (C_{11}^{7,i,j} - C_{12}^{7,i,j} + 2C_{22}^{7,i,j} + 2C_{23}^{7,i,j})(k_1, k_2) \\
&+ \frac{ie}{32\pi^2} Q_t \sum_{i=1,4} \sum_{j=1,2} G_1^{t\tilde{t}_j \tilde{\chi}_i^0} (C_{11}^{8,i,j} - C_{12}^{8,i,j} + 2C_{22}^{8,i,j} + 2C_{23}^{8,i,j})(k_1, k_2) \\
\\
g_{13}(k_1, k_2) &= \frac{-ie}{16\pi^2} \sum_{i=1,2} \sum_{j=1,2} F_1^{t\tilde{b}_j \tilde{\chi}_i^+} (C_0^{6,i,j} + C_{11}^{6,i,j} - C_{22}^{6,i,j} + C_{23}^{6,i,j})(k_1, k_2) \\
&+ \frac{ie}{32\pi^2} Q_b \sum_{i=1,2} \sum_{j=1,2} F_1^{t\tilde{b}_j \tilde{\chi}_i^+} (C_{12}^{7,i,j} - 2C_{22}^{7,i,j} + 2C_{23}^{7,i,j})(k_1, k_2) \\
&+ \frac{ie}{32\pi^2} Q_t \sum_{i=1,4} \sum_{j=1,2} G_1^{t\tilde{t}_j \tilde{\chi}_i^0} (C_{12}^{8,i,j} - 2C_{22}^{8,i,j} + 2C_{23}^{8,i,j})(k_1, k_2) \\
\\
g_{14}(k_1, k_2) &= \frac{ie}{16\pi^2} \sum_{i=1,2} \sum_{j=1,2} F_1^{t\tilde{b}_j \tilde{\chi}_i^+} (C_{12}^{6,i,j} + C_{22}^{6,i,j})(k_1, k_2) \\
&- \frac{ie}{32\pi^2} Q_b \sum_{i=1,2} \sum_{j=1,2} F_1^{t\tilde{b}_j \tilde{\chi}_i^+} (C_{12}^{7,i,j} + 2C_{22}^{7,i,j})(k_1, k_2) \\
&- \frac{ie}{32\pi^2} Q_t \sum_{i=1,4} \sum_{j=1,2} G_1^{t\tilde{t}_j \tilde{\chi}_i^0} (C_{12}^{8,i,j} + 2C_{22}^{8,i,j})(k_1, k_2)
\end{aligned}$$

$$\begin{aligned}
g_{15}(k_1, k_2) &= \frac{ie}{16\pi^2} \sum_{i=1,2} \sum_{j=1,2} F_2^{t\tilde{b}_j \tilde{\chi}_i^+} m_{\tilde{\chi}_i^+} (C_0^{6,i,j} + C_{11}^{6,i,j} - C_{12}^{6,i,j})(k_1, k_2) \\
&+ \frac{ie}{32\pi^2} Q_b \sum_{i=1,2} \sum_{j=1,2} F_2^{t\tilde{b}_j \tilde{\chi}_i^+} m_{\tilde{\chi}_i^+} (C_0^{7,i,j} + 2C_{11}^{7,i,j} - 2C_{12}^{7,i,j})(k_1, k_2) \\
&+ \frac{ie}{32\pi^2} Q_t \sum_{i=1,4} \sum_{j=1,2} G_2^{t\tilde{t}_j \tilde{\chi}_i^0} m_{\tilde{\chi}_i^0} (C_0^{8,i,j} + 2C_{11}^{8,i,j} - 2C_{12}^{8,i,j})(k_1, k_2)
\end{aligned}$$

$$\begin{aligned}
g_{16}(k_1, k_2) &= \frac{-ie}{16\pi^2} \sum_{i=1,2} \sum_{j=1,2} F_2^{t\tilde{b}_j \tilde{\chi}_i^+} m_{\tilde{\chi}_i^+} C_{12}^{6,i,j}(k_1, k_2) \\
&- \frac{ie}{32\pi^2} Q_b \sum_{i=1,2} \sum_{j=1,2} F_2^{t\tilde{b}_j \tilde{\chi}_i^+} m_{\tilde{\chi}_i^+} (C_0^{7,i,j} + 2C_{12}^{7,i,j})(k_1, k_2) \\
&- \frac{ie}{32\pi^2} Q_t \sum_{i=1,4} \sum_{j=1,2} G_2^{t\tilde{t}_j \tilde{\chi}_i^0} m_{\tilde{\chi}_i^0} (C_0^{8,i,j} + 2C_{12}^{8,i,j})(k_1, k_2)
\end{aligned}$$

$$g_{17}(k_1, k_2) = \frac{ie}{32\pi^2} \sum_{i=1,2} \sum_{j=1,2} F_1^{t\tilde{b}_j \tilde{\chi}_i^+} (C_0^{6,i,j} + C_{11}^{6,i,j})(k_1, k_2)$$

$$g_{18}(k_1, k_2) = g_{19}(k_1, k_2) = \frac{-ie}{32\pi^2} \sum_{i=1,2} \sum_{j=1,2} F_2^{t\tilde{b}_j \tilde{\chi}_i^+} m_{\tilde{\chi}_i^+} C_0^{6,i,j}(k_1, k_2)$$

$$\begin{aligned}
g_{20}(k_1, k_2) &= \frac{-ie}{32\pi^2} \sum_{i=1,2} \sum_{j=1,2} F_1^{t\tilde{b}_j \tilde{\chi}_i^+} ((\epsilon - 2)C_{24}^{6,i,j} + (k_1 \cdot k_1)(C_{11}^{6,i,j} - C_{12}^{6,i,j} + C_{21}^{6,i,j} \\
&+ C_{22}^{6,i,j} - 2C_{23}^{6,i,j}) + 2(k_1 \cdot k_2)(C_{22}^{6,i,j} - C_{23}^{6,i,j}) + (k_2 \cdot k_2)(C_{12}^{6,i,j} + C_{22}^{6,i,j}) \\
&- m_{\tilde{\chi}_i^+}^2 C_0^{6,i,j})(k_1, k_2) \\
&+ \frac{ie}{16\pi^2} Q_b \sum_{i=1,2} \sum_{j=1,2} F_1^{t\tilde{b}_j \tilde{\chi}_i^+} C_{24}^{7,i,j}(k_1, k_2) + \frac{ie}{16\pi^2} Q_t \sum_{i=1,4} \sum_{j=1,2} G_1^{t\tilde{t}_j \tilde{\chi}_i^0} C_{24}^{8,i,j}(k_1, k_2)
\end{aligned}$$

Then the form factors in the renormalized amplitude of the t-channel vertex diagrams in the process $\gamma\gamma \rightarrow t\bar{t}$ can be written as:

$$f_i^{v,\hat{t}} = 0 \quad (i = 2, 3, 6, 7, 9, 10, 12, 13, 16 \sim 22),$$

$$\begin{aligned} f_1^{v,\hat{t}} &= 2ieQ_t(p_1 \cdot p_3)A_t \{ m_t [g_{17}(p_1, p_3 - p_1) + g_{17}(p_1 - p_3, p_2)] \\ &\quad - g_{18}(p_1 - p_3, p_2) - g_{19}(p_1, p_3 - p_1) \}, \end{aligned}$$

$$f_4^{v,\hat{t}} = 2ieQ_t(p_1 \cdot p_3)A_t [g_{12}(p_1 - p_3, p_2) - g_{11}(p_1 - p_3, p_2)],$$

$$\begin{aligned} f_5^{v,\hat{t}} &= -2ieQ_t A_t \{ ie [C^+ + C^-] + m_t^2 (g_{11}(p_1, p_3 - p_1) - g_{12}(p_1, p_3 - p_1) \\ &\quad - g_{13}(p_1, p_3 - p_1) + g_{14}(p_1, p_3 - p_1) - g_{17}(p_1, p_3 - p_1) + g_{17}(p_1 - p_3, p_2)) \\ &\quad + (p_1 \cdot p_3)(g_{13}(p_1, p_3 - p_1) - g_{14}(p_1, p_3 - p_1) + 2g_{17}(p_1, p_3 - p_1)) \\ &\quad + m_t (g_{15}(p_1, p_3 - p_1) - g_{16}(p_1, p_3 - p_1) + g_{18}(p_1, p_3 - p_1) - g_{18}(p_1 - p_3, p_2) \\ &\quad - g_{19}(p_1, p_3 - p_1) - g_{19}(p_1 - p_3, p_2)) + g_{20}(p_1, p_3 - p_1) + g_{20}(p_1 - p_3, p_2) \}, \end{aligned}$$

$$\begin{aligned} f_8^{v,\hat{t}} &= 2f_{14}^{v,\hat{t}} = 2ieQ_t A_t \{ m_t [g_{11}(p_1 - p_3, p_2) - g_{12}(p_1 - p_3, p_2) - g_{13}(p_1 - p_3, p_2) \\ &\quad + g_{14}(p_1 - p_3, p_2) - 2g_{17}(p_1 - p_3, p_2)] + g_{15}(p_1 - p_3, p_2) - g_{16}(p_1 - p_3, p_2) \\ &\quad + 2g_{18}(p_1 - p_3, p_2) \}, \end{aligned}$$

$$\begin{aligned} f_{11}^{v,\hat{t}} &= -ieQ_t A_t \{ ie(C^+ + C^-) + m_t^2 (g_{17}(p_1, p_3 - p_1) + g_{17}(p_1 - p_3, p_2)) \\ &\quad - m_t (g_{18}(p_1, p_3 - p_1) + g_{18}(p_1 - p_3, p_2) + g_{19}(p_1, p_3 - p_1) \\ &\quad + g_{19}(p_1 - p_3, p_2)) + g_{20}(p_1, p_3 - p_1) + g_{20}(p_1 - p_3, p_2) \}, \end{aligned}$$

$$f_{15}^{v,\hat{t}} = f_{14}^{v,\hat{t}}(g_i(p_1 - p_3, p_2) \rightarrow g_i(p_1, p_3 - p_1)).$$

The form factors from the renormalized amplitude of t-channel box diagrams(Fig.1(c)) are expressed as:

$$\begin{aligned} f_1^{b,\hat{t}} &= \frac{-ie^2}{32\pi^2} \sum_{i=1,2} \sum_{j=1,2} (F_2^{t\tilde{b}_j \tilde{\chi}_i^+} m_{\tilde{\chi}_i^+} [2p_1 \cdot p_2 (D_{13}^{1,i,j} + D_{25}^{1,i,j} - D_{23}^{1,i,j}) \\ &\quad + 2p_1 \cdot p_3 (D_{11}^{1,i,j} + D_{12}^{1,i,j} + D_{23}^{1,i,j} + D_{24}^{1,i,j} - D_{25}^{1,i,j} - D_{26}^{1,i,j} - 2D_{13}^{1,i,j}) \\ &\quad + 2p_2 \cdot p_3 (D_{23}^{1,i,j} - D_{13}^{1,i,j} - D_{26}^{1,i,j}) + m_t^2 (2D_{13}^{1,i,j} + 2D_{25}^{1,i,j} - 2D_{11}^{1,i,j} - 2D_{23}^{1,i,j} \\ &\quad - D_0^{1,i,j} - D_{21}^{1,i,j}) + 2D_{27}^{1,i,j} + m_{\tilde{\chi}_i^+}^2 D_0^{1,i,j}] + F_1^{t\tilde{b}_j \tilde{\chi}_i^+} \{ 2p_1 \cdot p_2 m_t (D_{13}^{1,i,j} \right. \\ &\quad \left. - D_{21}^{1,i,j}) + 2D_{27}^{1,i,j} + m_{\tilde{\chi}_i^+}^2 D_0^{1,i,j} \} \} \end{aligned}$$

$$\begin{aligned}
& + D_{35}^{1,i,j} + 2D_{25}^{1,i,j} - D_{23}^{1,i,j} - D_{37}^{1,i,j}) + 2p_1 \cdot p_3 m_t (D_{11}^{1,i,j} + D_{12}^{1,i,j} + D_{21}^{1,i,j}) \\
& + D_{23}^{1,i,j} + D_{34}^{1,i,j} + D_{37}^{1,i,j} + 2D_{24}^{1,i,j} - 3D_{25}^{1,i,j} - D_{26}^{1,i,j} - D_{310}^{1,i,j} - D_{35}^{1,i,j} - 2D_{13}^{1,i,j}) \\
& + 2p_2 \cdot p_3 m_t (D_{23}^{1,i,j} + D_{37}^{1,i,j} - D_{13}^{1,i,j} - D_{25}^{1,i,j} - D_{26}^{1,i,j} - D_{310}^{1,i,j}) \\
& + m_t m_{\tilde{\chi}_i^+}^2 (D_0^{1,i,j} + D_{11}^{1,i,j}) + m_t [4D_{27}^{1,i,j} + (4-\epsilon)D_{311}^{1,i,j}] \\
& + m_t^3 (2D_{13}^{1,i,j} + 2D_{35}^{1,i,j} + 4D_{25}^{1,i,j} - 3D_{11}^{1,i,j} - 3D_{21}^{1,i,j} - 2D_{23}^{1,i,j} - 2D_{37}^{1,i,j} \\
& - D_0^{1,i,j} - D_{31}^{1,i,j})] - \frac{ie^2 Q_b^2}{16\pi^2} \sum_{i=1,2} \sum_{j=1,2} (F_1^{t\tilde{b}_j \tilde{\chi}_i^+} m_t D_{311}^{2,i,j} - F_2^{t\tilde{b}_j \tilde{\chi}_i^+} m_{\tilde{\chi}_i^+} D_{27}^{2,i,j}) \\
& - \frac{ie^2 Q_t^2}{16\pi^2} \sum_{i=1,4} \sum_{j=1,2} (G_1^{t\tilde{b}_j \tilde{\chi}_i^0} m_t D_{311}^{3,i,j} - G_2^{t\tilde{b}_j \tilde{\chi}_i^0} m_{\tilde{\chi}_i^0} D_{27}^{3,i,j}) \\
& - \frac{ie^2 Q_b}{16\pi^2} \sum_{i=1,2} \sum_{j=1,2} [F_2^{t\tilde{b}_j \tilde{\chi}_i^+} m_{\tilde{\chi}_i^+} D_{27}^{4,i,j} + F_1^{t\tilde{b}_j \tilde{\chi}_i^+} m_t (D_{27}^{4,i,j} + D_{312}^{4,i,j})] \\
f_2^{b,\hat{t}} & = \frac{ie^2}{16\pi^2} \sum_{i=1,2} \sum_{j=1,2} [F_1^{t\tilde{b}_j \tilde{\chi}_i^+} m_t (D_{27}^{1,i,j} + D_{311}^{1,i,j}) + F_2^{t\tilde{b}_j \tilde{\chi}_i^+} m_{\tilde{\chi}_i^+} D_{27}^{1,i,j}] \\
& - \frac{ie^2 Q_b^2}{16\pi^2} \sum_{i=1,2} \sum_{j=1,2} (F_1^{t\tilde{b}_j \tilde{\chi}_i^+} m_t D_{311}^{2,i,j} - F_2^{t\tilde{b}_j \tilde{\chi}_i^+} m_{\tilde{\chi}_i^+} D_{27}^{2,i,j}) \\
& - \frac{ie^2 Q_t^2}{16\pi^2} \sum_{i=1,4} \sum_{j=1,2} (G_1^{t\tilde{b}_j \tilde{\chi}_i^0} m_t D_{311}^{3,i,j} - G_2^{t\tilde{b}_j \tilde{\chi}_i^0} m_{\tilde{\chi}_i^0} D_{27}^{3,i,j}) \\
& - \frac{-ie^2 Q_b}{16\pi^2} \sum_{i=1,2} \sum_{j=1,2} [F_2^{t\tilde{b}_j \tilde{\chi}_i^+} m_{\tilde{\chi}_i^+} D_{27}^{4,i,j} + F_1^{t\tilde{b}_j \tilde{\chi}_i^+} m_t (D_{27}^{4,i,j} + D_{312}^{4,i,j})] \\
f_3^{b,\hat{t}} & = \frac{-ie^2}{16\pi^2} \sum_{i=1,2} \sum_{j=1,2} F_1^{t\tilde{b}_j \tilde{\chi}_i^+} [2p_1 \cdot p_2 (D_{25}^{1,i,j} + D_{35}^{1,i,j} + D_{39}^{1,i,j} - D_{26}^{1,i,j} - D_{310}^{1,i,j} - D_{37}^{1,i,j}) \\
& + 2p_1 \cdot p_3 (D_{24}^{1,i,j} + D_{26}^{1,i,j} + D_{34}^{1,i,j} + D_{37}^{1,i,j} + D_{38}^{1,i,j} - D_{22}^{1,i,j} - D_{25}^{1,i,j} - D_{35}^{1,i,j} \\
& - D_{36}^{1,i,j} - D_{39}^{1,i,j}) + 2p_2 \cdot p_3 (D_{26}^{1,i,j} + D_{37}^{1,i,j} + D_{38}^{1,i,j} - D_{25}^{1,i,j} - D_{310}^{1,i,j} - D_{39}^{1,i,j}) \\
& + m_t^2 (D_{12}^{1,i,j} + D_{34}^{1,i,j} + 2D_{24}^{1,i,j} + 2D_{25}^{1,i,j} + 2D_{35}^{1,i,j} + 2D_{39}^{1,i,j} - D_{11}^{1,i,j} - D_{31}^{1,i,j}) \\
& - 2D_{21}^{1,i,j} - 2D_{26}^{1,i,j} - 2D_{310}^{1,i,j} - 2D_{37}^{1,i,j}) + m_{\tilde{\chi}_i^+}^2 (D_{11}^{1,i,j} - D_{12}^{1,i,j}) \\
& + (4-\epsilon) (D_{311}^{1,i,j} - D_{312}^{1,i,j})] - \frac{ie^2 Q_b^2}{8\pi^2} \sum_{i=1,2} \sum_{j=1,2} F_1^{t\tilde{b}_j \tilde{\chi}_i^+} (D_{311}^{2,i,j} - D_{312}^{2,i,j})
\end{aligned}$$

$$-\frac{ie^2Q_t^2}{8\pi^2}\sum_{i=1,4}\sum_{j=1,2}G_1^{t\tilde{b}_j\tilde{\chi}_i^0}(D_{311}^{3,i,j}-D_{312}^{3,i,j})-\frac{ie^2Q_b}{8\pi^2}\sum_{i=1,2}\sum_{j=1,2}F_1^{t\tilde{b}_j\tilde{\chi}_i^+}(D_{312}^{4,i,j}-D_{311}^{4,i,j})$$

$$\begin{aligned} f_4^{b,\hat{t}} &= \frac{-ie^2}{16\pi^2}\sum_{i=1,2}\sum_{j=1,2}F_1^{t\tilde{b}_j\tilde{\chi}_i^+}\left[2p_1\cdot p_2(D_{23}^{1,i,j}+D_{37}^{1,i,j}+D_{39}^{1,i,j}-D_{26}^{1,i,j}-D_{310}^{1,i,j}-D_{33}^{1,i,j})\right. \\ &+ 2p_1\cdot p_3(2D_{26}^{1,i,j}+2D_{310}^{1,i,j}+D_{25}^{1,i,j}+D_{33}^{1,i,j}+D_{38}^{1,i,j}-2D_{23}^{1,i,j}-2D_{39}^{1,i,j}-D_{22}^{1,i,j} \\ &- D_{36}^{1,i,j}-D_{37}^{1,i,j})+2p_2\cdot p_3(D_{26}^{1,i,j}+D_{33}^{1,i,j}+D_{38}^{1,i,j}-2D_{39}^{1,i,j}-D_{23}^{1,i,j}) \\ &+ m_t^2(D_{12}^{1,i,j}+D_{34}^{1,i,j}+2D_{23}^{1,i,j}+2D_{24}^{1,i,j}+2D_{37}^{1,i,j}+2D_{39}^{1,i,j}-D_{13}^{1,i,j}-D_{35}^{1,i,j}) \\ &- 2D_{25}^{1,i,j}-2D_{26}^{1,i,j}-2D_{310}^{1,i,j}-2D_{33}^{1,i,j})+m_{\tilde{\chi}_i^+}^2(D_{13}^{1,i,j}-D_{12}^{1,i,j}) \\ &+ (6-\epsilon)D_{313}^{1,i,j}-2D_{27}^{1,i,j}-(4-\epsilon)D_{312}^{1,i,j}\Big]+\frac{ie^2Q_b^2}{8\pi^2}\sum_{i=1,2}\sum_{j=1,2}F_1^{t\tilde{b}_j\tilde{\chi}_i^+}(D_{27}^{2,i,j}+D_{312}^{2,i,j}) \\ &+ \frac{ie^2Q_t^2}{8\pi^2}\sum_{i=1,4}\sum_{j=1,2}G_1^{t\tilde{b}_j\tilde{\chi}_i^0}(D_{27}^{3,i,j}+D_{312}^{3,i,j})+\frac{ie^2Q_b}{8\pi^2}\sum_{i=1,2}\sum_{j=1,2}F_1^{t\tilde{b}_j\tilde{\chi}_i^+}D_{311}^{4,i,j} \end{aligned}$$

$$\begin{aligned} f_5^{b,\hat{t}} &= \frac{-ie^2}{16\pi^2}\sum_{i=1,2}\sum_{j=1,2}\left\{2F_2^{t\tilde{b}_j\tilde{\chi}_i^+}m_tm_{\tilde{\chi}_i^+}(D_0^{1,i,j}+D_{11}^{1,i,j}-D_{13}^{1,i,j})\right. \\ &+ F_1^{t\tilde{b}_j\tilde{\chi}_i^+}\left[2p_2\cdot p_3(D_{25}^{1,i,j}-D_{26}^{1,i,j})+m_t^2(D_0^{1,i,j}+D_{21}^{1,i,j}+2D_{11}^{1,i,j}-2D_{13}^{1,i,j}\right. \\ &- 2D_{25}^{1,i,j})+m_{\tilde{\chi}_i^+}^2D_0^{1,i,j}+2(D_{313}^{1,i,j}-D_{311}^{1,i,j})\Big]\Big\}-\frac{ie^2Q_b^2}{8\pi^2}\sum_{i=1,2}\sum_{j=1,2}F_1^{t\tilde{b}_j\tilde{\chi}_i^+}(D_{27}^{2,i,j}+D_{311}^{2,i,j}) \\ &- D_{313}^{2,i,j})-\frac{ie^2Q_t^2}{8\pi^2}\sum_{i=1,4}\sum_{j=1,2}G_1^{t\tilde{b}_j\tilde{\chi}_i^0}(D_{27}^{3,i,j}+D_{311}^{3,i,j}-D_{313}^{3,i,j})-\frac{ie^2Q_b}{16\pi^2}\sum_{i=1,2}\sum_{j=1,2}\left\{2F_2^{t\tilde{b}_j\tilde{\chi}_i^+}m_tm_{\tilde{\chi}_i^+}(D_{13}^{4,i,j}-D_{12}^{4,i,j})+F_1^{t\tilde{b}_j\tilde{\chi}_i^+}\left[2p_1\cdot p_2(2D_{39}^{4,i,j}-D_{33}^{4,i,j}-D_{38}^{4,i,j}\right.\right. \\ &+ 2p_1\cdot p_3(2D_{26}^{4,i,j}+2D_{310}^{4,i,j}+D_{33}^{4,i,j}+D_{38}^{4,i,j}-2D_{39}^{4,i,j}-D_{22}^{4,i,j}-D_{23}^{4,i,j}-D_{36}^{4,i,j} \\ &- D_{37}^{4,i,j})+2p_2\cdot p_3(D_{310}^{4,i,j}+D_{33}^{4,i,j}-D_{37}^{4,i,j}-D_{39}^{4,i,j})+m_t^2(D_{13}^{4,i,j}+D_{32}^{4,i,j}) \\ &+ 4D_{39}^{4,i,j}-3D_{38}^{4,i,j}-D_{12}^{4,i,j}-2D_{33}^{4,i,j})+m_{\tilde{\chi}_i^+}^2(D_{13}^{4,i,j}-D_{12}^{4,i,j}) \\ &\left.\left.+ (4-\epsilon)(D_{313}^{4,i,j}-D_{312}^{4,i,j})\right]\right\} \end{aligned}$$

$$\begin{aligned}
f_6^{b,\hat{t}} = & \frac{-ie^2}{16\pi^2} \sum_{i=1,2} \sum_{j=1,2} \left\{ -2F_2^{t\tilde{b}_j\tilde{\chi}_i^+} m_t m_{\tilde{\chi}_i^+} D_{13}^{1,i,j} + F_1^{t\tilde{b}_j\tilde{\chi}_i^+} [2p_1 \cdot p_2 (D_{33}^{1,i,j} - D_{37}^{1,i,j}) \right. \\
& + 2p_1 \cdot p_3 (D_{23}^{1,i,j} + D_{37}^{1,i,j} + D_{39}^{1,i,j} - D_{25}^{1,i,j} - D_{310}^{1,i,j} - D_{33}^{1,i,j}) \\
& + 2p_2 \cdot p_3 (D_{39}^{1,i,j} - D_{33}^{1,i,j}) + m_t^2 (D_{35}^{1,i,j} + 2D_{33}^{1,i,j} - D_{13}^{1,i,j} - 2D_{37}^{1,i,j}) \\
& \left. - m_{\tilde{\chi}_i^+}^2 D_{13}^{1,i,j} - (4-\epsilon) D_{313}^{1,i,j}] \right\} + \frac{ie^2 Q_b^2}{8\pi^2} \sum_{i=1,2} \sum_{j=1,2} F_1^{t\tilde{b}_j\tilde{\chi}_i^+} D_{313}^{2,i,j} + \frac{ie^2 Q_t^2}{8\pi^2} \sum_{i=1,4} \sum_{j=1,2} \\
& G_1^{t\tilde{b}_j\tilde{\chi}_i^0} D_{313}^{3,i,j} - \frac{ie^2 Q_b}{16\pi^2} \sum_{i=1,2} \sum_{j=1,2} \left\{ 2F_2^{t\tilde{b}_j\tilde{\chi}_i^+} m_t m_{\tilde{\chi}_i^+} D_{13}^{4,i,j} + F_1^{t\tilde{b}_j\tilde{\chi}_i^+} [2p_1 \cdot p_2 (D_{39}^{4,i,j} \right. \\
& - D_{33}^{4,i,j}) + 2p_1 \cdot p_3 (D_{26}^{4,i,j} + D_{310}^{4,i,j} + D_{33}^{4,i,j} - D_{23}^{4,i,j} - D_{37}^{4,i,j} - D_{39}^{4,i,j}) \\
& + 2p_2 \cdot p_3 (D_{33}^{4,i,j} - D_{37}^{4,i,j}) + m_t^2 (D_{13}^{4,i,j} + 2D_{39}^{4,i,j} - D_{38}^{4,i,j} - 2D_{33}^{4,i,j}) \\
& \left. + m_{\tilde{\chi}_i^+}^2 D_{13}^{4,i,j} + (4-\epsilon) D_{313}^{4,i,j}] \right\}
\end{aligned}$$

$$\begin{aligned}
f_7^{b,\hat{t}} = & \frac{-ie^2}{8\pi^2} \sum_{i=1,2} \sum_{j=1,2} \left[F_2^{t\tilde{b}_j\tilde{\chi}_i^+} m_{\tilde{\chi}_i^+} (D_{11}^{1,i,j} + D_{21}^{1,i,j} + D_{26}^{1,i,j} - D_{12}^{1,i,j} - D_{24}^{1,i,j} - D_{25}^{1,i,j}) \right. \\
& + F_1^{t\tilde{b}_j\tilde{\chi}_i^+} m_t (2D_{21}^{1,i,j} + D_{11}^{1,i,j} + D_{26}^{1,i,j} + D_{310}^{1,i,j} + D_{31}^{1,i,j} - 2D_{24}^{1,i,j} - D_{12}^{1,i,j} \\
& - D_{25}^{1,i,j} - D_{34}^{1,i,j} - D_{35}^{1,i,j}) \left. - \frac{ie^2 Q_b^2}{8\pi^2} \sum_{i=1,2} \sum_{j=1,2} \left[F_2^{t\tilde{b}_j\tilde{\chi}_i^+} m_{\tilde{\chi}_i^+} (D_{11}^{2,i,j} + D_{21}^{2,i,j} + D_{26}^{2,i,j} \right. \right. \\
& - D_{12}^{2,i,j} - D_{24}^{2,i,j} - D_{25}^{2,i,j}) + F_1^{t\tilde{b}_j\tilde{\chi}_i^+} m_t (D_{24}^{2,i,j} + D_{34}^{2,i,j} + D_{35}^{2,i,j} - D_{21}^{2,i,j} \\
& - D_{310}^{2,i,j} - D_{31}^{2,i,j}) \left. - \frac{ie^2 Q_t^2}{8\pi^2} \sum_{i=1,4} \sum_{j=1,2} \left[G_2^{t\tilde{b}_j\tilde{\chi}_i^0} m_{\tilde{\chi}_i^0} (D_{11}^{3,i,j} + D_{21}^{3,i,j} + D_{26}^{3,i,j} - D_{12}^{3,i,j} \right. \right. \\
& - D_{24}^{3,i,j} - D_{25}^{3,i,j}) + G_1^{t\tilde{b}_j\tilde{\chi}_i^0} m_t (D_{24}^{3,i,j} + D_{34}^{3,i,j} + D_{35}^{3,i,j} - D_{21}^{3,i,j} - D_{310}^{3,i,j} \\
& - D_{31}^{3,i,j}) \left. - \frac{ie^2 Q_b}{8\pi^2} \sum_{i=1,2} \sum_{j=1,2} \left[F_2^{t\tilde{b}_j\tilde{\chi}_i^+} m_{\tilde{\chi}_i^+} (D_{24}^{4,i,j} + D_{26}^{4,i,j} - D_{22}^{4,i,j} - D_{25}^{4,i,j}) \right. \right. \\
& + F_1^{t\tilde{b}_j\tilde{\chi}_i^+} m_t (D_{24}^{4,i,j} + D_{26}^{4,i,j} + D_{36}^{4,i,j} + D_{38}^{4,i,j} - D_{22}^{4,i,j} - D_{25}^{4,i,j} - D_{310}^{4,i,j} \\
& \left. - D_{32}^{4,i,j}) \right]
\end{aligned}$$

$$\begin{aligned}
f_8^{b,\hat{t}} = & \frac{-ie^2}{8\pi^2} \sum_{i=1,2} \sum_{j=1,2} \left[F_2^{t\tilde{b}_j\tilde{\chi}_i^+} m_{\tilde{\chi}_i^+} (-D_{12}^{1,i,j} + D_{26}^{1,i,j} - D_{24}^{1,i,j}) + F_1^{t\tilde{b}_j\tilde{\chi}_i^+} m_t (D_{26}^{1,i,j} \right. \\
& + D_{310}^{1,i,j} - 2D_{24}^{1,i,j} - D_{12}^{1,i,j} - D_{34}^{1,i,j}) \Big] - \frac{ie^2 Q_b^2}{8\pi^2} \sum_{i=1,2} \sum_{j=1,2} \left[F_2^{t\tilde{b}_j\tilde{\chi}_i^+} m_{\tilde{\chi}_i^+} (D_{13}^{2,i,j} + D_{26}^{2,i,j} \right. \\
& - D_0^{2,i,j} - D_{11}^{2,i,j} - D_{12}^{2,i,j} - D_{24}^{2,i,j}) + F_1^{t\tilde{b}_j\tilde{\chi}_i^+} m_t (D_{11}^{2,i,j} + D_{21}^{2,i,j} + D_{24}^{2,i,j} \\
& + D_{34}^{2,i,j} - D_{25}^{2,i,j} - D_{310}^{2,i,j}) \Big] - \frac{ie^2 Q_t^2}{8\pi^2} \sum_{i=1,4} \sum_{j=1,2} \left[G_2^{t\tilde{t}_j\tilde{\chi}_i^0} m_{\tilde{\chi}_i^0} (D_{13}^{3,i,j} + D_{26}^{3,i,j} - D_0^{3,i,j} \right. \\
& - D_{11}^{3,i,j} - D_{12}^{3,i,j} - D_{24}^{3,i,j}) + G_1^{t\tilde{t}_j\tilde{\chi}_i^0} m_t (D_{11}^{3,i,j} + D_{21}^{3,i,j} + D_{24}^{3,i,j} + D_{34}^{3,i,j} \\
& - D_{25}^{3,i,j} - D_{310}^{3,i,j}) \Big] - \frac{ie^2 Q_b}{8\pi^2} \sum_{i=1,2} \sum_{j=1,2} \left[F_2^{t\tilde{b}_j\tilde{\chi}_i^+} m_{\tilde{\chi}_i^+} (D_{24}^{4,i,j} - D_{25}^{4,i,j}) \right. \\
& + F_1^{t\tilde{b}_j\tilde{\chi}_i^+} m_t (D_{24}^{4,i,j} + D_{36}^{4,i,j} - D_{25}^{4,i,j} - D_{310}^{4,i,j}) \Big]
\end{aligned}$$

$$\begin{aligned}
f_9^{b,\hat{t}} = & \frac{-ie^2}{8\pi^2} \sum_{i=1,2} \sum_{j=1,2} \left[F_2^{t\tilde{b}_j\tilde{\chi}_i^+} m_{\tilde{\chi}_i^+} (D_{26}^{1,i,j} - D_{25}^{1,i,j}) + F_1^{t\tilde{b}_j\tilde{\chi}_i^+} m_t (D_{26}^{1,i,j} + D_{310}^{1,i,j} \right. \\
& - D_{25}^{1,i,j} - D_{35}^{1,i,j}) \Big] - \frac{ie^2 Q_b^2}{8\pi^2} \sum_{i=1,2} \sum_{j=1,2} \left[F_2^{t\tilde{b}_j\tilde{\chi}_i^+} m_{\tilde{\chi}_i^+} (D_{26}^{2,i,j} - D_{25}^{2,i,j}) \right. \\
& + F_1^{t\tilde{b}_j\tilde{\chi}_i^+} m_t (D_{35}^{2,i,j} - D_{310}^{2,i,j}) \Big] - \frac{ie^2 Q_t^2}{8\pi^2} \sum_{i=1,4} \sum_{j=1,2} \left[G_2^{t\tilde{t}_j\tilde{\chi}_i^0} m_{\tilde{\chi}_i^0} (D_{26}^{3,i,j} - D_{25}^{3,i,j}) \right. \\
& + G_1^{t\tilde{t}_j\tilde{\chi}_i^0} m_t (D_{35}^{3,i,j} - D_{310}^{3,i,j}) \Big] - \frac{ie^2 Q_b}{8\pi^2} \sum_{i=1,2} \sum_{j=1,2} \left[F_2^{t\tilde{b}_j\tilde{\chi}_i^+} m_{\tilde{\chi}_i^+} (D_{26}^{4,i,j} - D_{25}^{4,i,j}) \right. \\
& + F_1^{t\tilde{b}_j\tilde{\chi}_i^+} m_t (D_{26}^{4,i,j} + D_{38}^{4,i,j} - D_{25}^{4,i,j} - D_{310}^{4,i,j}) \Big]
\end{aligned}$$

$$\begin{aligned}
f_{10}^{b,\hat{t}} = & \frac{-ie^2}{8\pi^2} \sum_{i=1,2} \sum_{j=1,2} \left[F_2^{t\tilde{b}_j\tilde{\chi}_i^+} m_{\tilde{\chi}_i^+} D_{26}^{1,i,j} + F_1^{t\tilde{b}_j\tilde{\chi}_i^+} m_t (D_{26}^{1,i,j} + D_{310}^{1,i,j}) \right] \\
& - \frac{ie^2 Q_b^2}{8\pi^2} \sum_{i=1,2} \sum_{j=1,2} \left[F_2^{t\tilde{b}_j\tilde{\chi}_i^+} m_{\tilde{\chi}_i^+} (D_{13}^{2,i,j} + D_{26}^{2,i,j}) - F_1^{t\tilde{b}_j\tilde{\chi}_i^+} m_t (D_{25}^{2,i,j} + D_{310}^{2,i,j}) \right]
\end{aligned}$$

$$\begin{aligned}
& - \frac{ie^2 Q_t^2}{8\pi^2} \sum_{i=1,4} \sum_{j=1,2} \left[G_2^{t\tilde{b}_j \tilde{\chi}_i^0} m_{\tilde{\chi}_i^0} (D_{13}^{3,i,j} + D_{26}^{3,i,j}) - G_1^{t\tilde{b}_j \tilde{\chi}_i^0} m_t (D_{25}^{3,i,j} + D_{310}^{3,i,j}) \right] \\
& + \frac{ie^2 Q_b}{8\pi^2} \sum_{i=1,2} \sum_{j=1,2} \left[F_2^{t\tilde{b}_j \tilde{\chi}_i^+} m_{\tilde{\chi}_i^+} D_{25}^{4,i,j} + F_1^{t\tilde{b}_j \tilde{\chi}_i^+} m_t (D_{25}^{4,i,j} + D_{310}^{4,i,j}) \right]
\end{aligned}$$

$$\begin{aligned}
f_{11}^{b,\hat{t}} &= \frac{-ie^2}{32\pi^2} \sum_{i=1,2} \sum_{j=1,2} \left\{ 2F_2^{t\tilde{b}_j \tilde{\chi}_i^+} m_t m_{\tilde{\chi}_i^+} D_0^{1,i,j} + F_1^{t\tilde{b}_j \tilde{\chi}_i^+} [2p_1 \cdot p_2 (D_{25}^{1,i,j} + D_{37}^{1,i,j}) \right. \\
&\quad + D_{39}^{1,i,j} - D_{26}^{1,i,j} - D_{310}^{1,i,j} - D_{33}^{1,i,j}) + 2p_1 \cdot p_3 (D_{33}^{1,i,j} + D_{38}^{1,i,j} + 2D_{26}^{1,i,j} + 2D_{310}^{1,i,j} \\
&\quad - D_{22}^{1,i,j} - D_{23}^{1,i,j} - D_{36}^{1,i,j} - D_{39}^{1,i,j} - 2D_{39}^{1,i,j}) + 2p_2 \cdot p_3 (D_{33}^{1,i,j} + D_{38}^{1,i,j} - 2D_{39}^{1,i,j}) \\
&\quad + m_t^2 (2D_{24}^{1,i,j} + 2D_{37}^{1,i,j} + 2D_{39}^{1,i,j} + D_0^{1,i,j} + D_{12}^{1,i,j} + D_{34}^{1,i,j} - 2D_{26}^{1,i,j} - 2D_{310}^{1,i,j} \\
&\quad - 2D_{33}^{1,i,j} - D_{13}^{1,i,j} - D_{21}^{1,i,j} - D_{35}^{1,i,j}) + m_{\tilde{\chi}_i^+}^2 (D_0^{1,i,j} + D_{13}^{1,i,j} - D_{12}^{1,i,j}) \\
&\quad \left. + (4 - \epsilon) (D_{313}^{1,i,j} - D_{312}^{1,i,j}) \right] \} + \frac{-ie^2 Q_b^2}{16\pi^2} \sum_{i=1,2} \sum_{j=1,2} F_1^{t\tilde{b}_j \tilde{\chi}_i^+} (D_{313}^{2,i,j} - D_{312}^{2,i,j}) \\
&+ \frac{-ie^2 Q_t^2}{16\pi^2} \sum_{i=1,4} \sum_{j=1,2} G_1^{t\tilde{b}_j \tilde{\chi}_i^0} (D_{313}^{3,i,j} - D_{312}^{3,i,j}) + \frac{-ie^2 Q_b}{16\pi^2} \sum_{i=1,2} \sum_{j=1,2} F_1^{t\tilde{b}_j \tilde{\chi}_i^+} (D_{313}^{4,i,j} - D_{311}^{4,i,j}) \\
f_{12}^{b,\hat{t}} &= \frac{-ie^2}{16\pi^2} \sum_{i=1,2} \sum_{j=1,2} F_1^{t\tilde{b}_j \tilde{\chi}_i^+} (D_{27}^{1,i,j} + D_{312}^{1,i,j} - D_{313}^{1,i,j}) + \frac{-ie^2 Q_b^2}{16\pi^2} \sum_{i=1,2} \sum_{j=1,2} F_1^{t\tilde{b}_j \tilde{\chi}_i^+} \\
&\quad (D_{313}^{2,i,j} - D_{312}^{2,i,j}) + \frac{-ie^2 Q_t^2}{16\pi^2} \sum_{i=1,4} \sum_{j=1,2} G_1^{t\tilde{b}_j \tilde{\chi}_i^0} (D_{313}^{3,i,j} - D_{312}^{3,i,j}) \\
&+ \frac{-ie^2 Q_b}{16\pi^2} \sum_{i=1,2} \sum_{j=1,2} F_1^{t\tilde{b}_j \tilde{\chi}_i^+} (D_{313}^{4,i,j} - D_{27}^{4,i,j} - D_{311}^{4,i,j}) \\
f_{13}^{b,\hat{t}} &= \frac{-ie^2}{16\pi^2} \sum_{i=1,2} \sum_{j=1,2} \left[F_2^{t\tilde{b}_j \tilde{\chi}_i^+} m_{\tilde{\chi}_i^+} (D_{11}^{1,i,j} - D_{12}^{1,i,j}) + F_1^{t\tilde{b}_j \tilde{\chi}_i^+} m_t (D_{11}^{1,i,j} + D_{21}^{1,i,j} \right. \\
&\quad \left. - D_{12}^{1,i,j} - D_{24}^{1,i,j}) \right] \\
f_{14}^{b,\hat{t}} &= \frac{ie^2}{16\pi^2} \sum_{i=1,2} \sum_{j=1,2} \left[F_2^{t\tilde{b}_j \tilde{\chi}_i^+} m_{\tilde{\chi}_i^+} D_{12}^{1,i,j} + F_1^{t\tilde{b}_j \tilde{\chi}_i^+} m_t (D_{12}^{1,i,j} + D_{24}^{1,i,j}) \right]
\end{aligned}$$

$$\begin{aligned}
f_{15}^{b,\hat{t}} = & \frac{-ie^2}{16\pi^2} \sum_{i=1,2} \sum_{j=1,2} \left[F_2^{t\tilde{b}_j\tilde{\chi}_i^+} m_{\tilde{\chi}_i^+} (D_{13}^{1,i,j} - D_{11}^{1,i,j}) + F_1^{t\tilde{b}_j\tilde{\chi}_i^+} m_t (D_{13}^{1,i,j} + D_{25}^{1,i,j} \right. \\
& - D_{11}^{1,i,j} - D_{21}^{1,i,j}) \Big] - \frac{ie^2 Q_b}{16\pi^2} \sum_{i=1,2} \sum_{j=1,2} \left[F_2^{t\tilde{b}_j\tilde{\chi}_i^+} m_{\tilde{\chi}_i^+} (D_{12}^{4,i,j} - D_{13}^{4,i,j}) \right. \\
& \left. + F_1^{t\tilde{b}_j\tilde{\chi}_i^+} m_t (D_{12}^{4,i,j} + D_{22}^{4,i,j} - D_{13}^{4,i,j} - D_{26}^{4,i,j}) \right]
\end{aligned}$$

$$\begin{aligned}
f_{16}^{b,\hat{t}} = & \frac{-ie^2}{16\pi^2} \sum_{i=1,2} \sum_{j=1,2} \left[F_2^{t\tilde{b}_j\tilde{\chi}_i^+} m_{\tilde{\chi}_i^+} D_{13}^{1,i,j} + F_1^{t\tilde{b}_j\tilde{\chi}_i^+} m_t (D_{13}^{1,i,j} + D_{25}^{1,i,j}) \right] \\
& + \frac{ie^2 Q_b}{16\pi^2} \sum_{i=1,2} \sum_{j=1,2} \left[F_2^{t\tilde{b}_j\tilde{\chi}_i^+} m_{\tilde{\chi}_i^+} D_{13}^{4,i,j} + F_1^{t\tilde{b}_j\tilde{\chi}_i^+} m_t (D_{13}^{4,i,j} + D_{26}^{4,i,j}) \right]
\end{aligned}$$

$$\begin{aligned}
f_{17}^{b,\hat{t}} = & \frac{-ie^2}{8\pi^2} \sum_{i=1,2} \sum_{j=1,2} F_1^{t\tilde{b}_j\tilde{\chi}_i^+} (D_{22}^{1,i,j} + D_{25}^{1,i,j} + D_{35}^{1,i,j} + D_{36}^{1,i,j} + D_{39}^{1,i,j} - D_{24}^{1,i,j} - D_{26}^{1,i,j} \\
& - D_{34}^{1,i,j} - D_{37}^{1,i,j} - D_{38}^{1,i,j}) - \frac{ie^2 Q_b^2}{8\pi^2} \sum_{i=1,2} \sum_{j=1,2} F_1^{t\tilde{b}_j\tilde{\chi}_i^+} (D_{24}^{2,i,j} + D_{26}^{2,i,j} + D_{34}^{2,i,j} + D_{37}^{2,i,j} \\
& + D_{38}^{2,i,j} - D_{22}^{2,i,j} - D_{25}^{2,i,j} - D_{35}^{2,i,j} - D_{36}^{2,i,j} - D_{39}^{2,i,j}) - \frac{ie^2 Q_t^2}{8\pi^2} \sum_{i=1,4} \sum_{j=1,2} G_1^{t\tilde{t}_j\tilde{\chi}_i^0} (D_{24}^{3,i,j} \\
& + D_{26}^{3,i,j} + D_{34}^{3,i,j} + D_{37}^{3,i,j} + D_{38}^{3,i,j} - D_{22}^{3,i,j} - D_{25}^{3,i,j} - D_{35}^{3,i,j} - D_{36}^{3,i,j} - D_{39}^{3,i,j}) \\
& - \frac{ie^2 Q_b}{8\pi^2} \sum_{i=1,2} \sum_{j=1,2} F_1^{t\tilde{b}_j\tilde{\chi}_i^+} (D_{22}^{4,i,j} + D_{25}^{4,i,j} + D_{35}^{4,i,j} + D_{36}^{4,i,j} + D_{39}^{4,i,j} - D_{24}^{4,i,j} - D_{26}^{4,i,j} \\
& - D_{34}^{4,i,j} - D_{37}^{4,i,j} - D_{38}^{4,i,j})
\end{aligned}$$

$$\begin{aligned}
f_{18}^{b,\hat{t}} = & \frac{-ie^2}{8\pi^2} \sum_{i=1,2} \sum_{j=1,2} F_1^{t\tilde{b}_j\tilde{\chi}_i^+} (D_{22}^{1,i,j} + D_{23}^{1,i,j} + D_{36}^{1,i,j} + D_{39}^{1,i,j} - D_{25}^{1,i,j} - D_{26}^{1,i,j} - D_{310}^{1,i,j} \\
& - D_{38}^{1,i,j}) - \frac{ie^2 Q_b^2}{8\pi^2} \sum_{i=1,2} \sum_{j=1,2} F_1^{t\tilde{b}_j\tilde{\chi}_i^+} (2D_{26}^{2,i,j} + D_{13}^{2,i,j} + D_{25}^{2,i,j} + D_{310}^{2,i,j} + D_{38}^{2,i,j} - D_{12}^{2,i,j})
\end{aligned}$$

$$\begin{aligned}
& - D_{22}^{2,i,j} - D_{23}^{2,i,j} - D_{24}^{2,i,j} - D_{36}^{2,i,j} - D_{39}^{2,i,j}) - \frac{ie^2 Q_t^2}{8\pi^2} \sum_{i=1,4} \sum_{j=1,2} G_1^{t\tilde{t}_j \tilde{\chi}_i^0} (2D_{26}^{3,i,j} + D_{13}^{3,i,j} \\
& + D_{25}^{3,i,j} + D_{310}^{3,i,j} + D_{38}^{3,i,j} - D_{12}^{3,i,j} - D_{22}^{3,i,j} - D_{23}^{3,i,j} - D_{24}^{3,i,j} - D_{36}^{3,i,j} - D_{39}^{3,i,j}) \\
& - \frac{ie^2 Q_b}{8\pi^2} \sum_{i=1,2} \sum_{j=1,2} F_1^{t\tilde{b}_j \tilde{\chi}_i^+} (D_{25}^{4,i,j} + D_{26}^{4,i,j} + D_{310}^{4,i,j} + D_{35}^{4,i,j} - D_{23}^{4,i,j} - D_{24}^{4,i,j} - D_{34}^{4,i,j} \\
& - D_{37}^{4,i,j})
\end{aligned}$$

$$\begin{aligned}
f_{19}^{b,\hat{t}} & = \frac{-ie^2}{8\pi^2} \sum_{i=1,2} \sum_{j=1,2} F_1^{t\tilde{b}_j \tilde{\chi}_i^+} (D_{25}^{1,i,j} + D_{310}^{1,i,j} + D_{39}^{1,i,j} - D_{26}^{1,i,j} - D_{37}^{1,i,j} - D_{38}^{1,i,j}) \\
& - \frac{ie^2 Q_b^2}{8\pi^2} \sum_{i=1,2} \sum_{j=1,2} F_1^{t\tilde{b}_j \tilde{\chi}_i^+} (D_{37}^{2,i,j} + D_{38}^{2,i,j} - D_{39}^{2,i,j} - D_{310}^{2,i,j}) - \frac{ie^2 Q_t^2}{8\pi^2} \sum_{i=1,4} \sum_{j=1,2} G_1^{t\tilde{t}_j \tilde{\chi}_i^0} \\
& (D_{37}^{3,i,j} + D_{38}^{3,i,j} - D_{39}^{3,i,j} - D_{310}^{3,i,j}) - \frac{ie^2 Q_b}{8\pi^2} \sum_{i=1,2} \sum_{j=1,2} F_1^{t\tilde{b}_j \tilde{\chi}_i^+} (D_{25}^{4,i,j} + D_{35}^{4,i,j} + D_{39}^{4,i,j} \\
& - D_{26}^{4,i,j} - D_{310}^{4,i,j} - D_{37}^{4,i,j})
\end{aligned}$$

$$\begin{aligned}
f_{20}^{b,\hat{t}} & = \frac{-ie^2}{8\pi^2} \sum_{i=1,2} \sum_{j=1,2} F_1^{t\tilde{b}_j \tilde{\chi}_i^+} (D_{23}^{1,i,j} + D_{39}^{1,i,j} - D_{26}^{1,i,j} - D_{38}^{1,i,j}) - \frac{ie^2 Q_b^2}{8\pi^2} \sum_{i=1,2} \sum_{j=1,2} F_1^{t\tilde{b}_j \tilde{\chi}_i^+} \\
& (D_{26}^{2,i,j} + D_{38}^{2,i,j} - D_{23}^{2,i,j} - D_{39}^{2,i,j}) - \frac{ie^2 Q_t^2}{8\pi^2} \sum_{i=1,4} \sum_{j=1,2} G_1^{t\tilde{t}_j \tilde{\chi}_i^0} (D_{26}^{3,i,j} + D_{38}^{3,i,j} - D_{23}^{3,i,j} \\
& - D_{39}^{3,i,j}) - \frac{ie^2 Q_b}{8\pi^2} \sum_{i=1,2} \sum_{j=1,2} F_1^{t\tilde{b}_j \tilde{\chi}_i^+} (D_{25}^{4,i,j} + D_{35}^{4,i,j} - D_{23}^{4,i,j} - D_{37}^{4,i,j})
\end{aligned}$$

$$f_{21,22}^{b,\hat{t}} = 0.$$

The form factors in the renormalized amplitude of the quartic interaction diagrams in Fig.1(d) have the form as:

$$f_1^q = f_2^q = \frac{-ie^2}{32\pi^2} \left[Q_b^2 \sum_{i=1,2} \sum_{j=1,2} (F_2^{t\tilde{b}_j \tilde{\chi}_i^+} m_{\tilde{\chi}_i^+} C_0^{1,i,j} - F_1^{t\tilde{b}_j \tilde{\chi}_i^+} m_t C_{11}^{1,i,j}) \right]$$

$$\begin{aligned}
& + Q_t^2 \sum_{i=1,4} \sum_{j=1,2} (G_2^{t\tilde{t}_j\tilde{\chi}_i^0} m_{\tilde{\chi}_i^0} C_0^{2,i,j} - G_1^{t\tilde{t}_j\tilde{\chi}_i^0} m_t C_{11}^{2,i,j}) \\
& + 2iQ_b^2 \sum_{k=1,2} \bar{B}_0^{1,k} (A_h V_{h^0tt} V_{h^0\tilde{b}_k\tilde{b}_k} + A_H V_{H^0tt} V_{H^0\tilde{b}_k\tilde{b}_k}) \\
& + 2iQ_t^2 \sum_{k=1,2} \bar{B}_0^{2,k} (A_h V_{h^0tt} V_{h^0\tilde{t}_k\tilde{t}_k} + A_H V_{H^0tt} V_{H^0\tilde{t}_k\tilde{t}_k}) \Big] \\
& f_i^q = 0, \quad (i = 3 \sim 22)
\end{aligned}$$

The form factors in the renormalized amplitude from the t-channel triangle diagrams depicted in Fig.1(e), are listed below:

$$\begin{aligned}
f_1^{tr,\hat{t}} &= f_2^{tr,\hat{t}} = \frac{e^2}{8\pi^2} \sum_{k=1,2} m_{\tilde{\chi}_k^+} \left[2p_1 \cdot p_2 C_{22}^{3,k} + (p_1 \cdot p_3 + p_2 \cdot p_3) \cdot \right. \\
&\quad (C_0^{3,k} - 2C_{23}^{3,k}) + \epsilon \bar{C}_{24}^{3,k} + 2m_t^2 C_{22}^{3,k} - m_{\tilde{\chi}_k^+}^2 C_0^{3,k} \Big] \cdot \\
&\quad (A_h V_{h^0tt} V_{h^0\tilde{\chi}_k^+\tilde{\chi}_k^+}^s + A_H V_{H^0tt} V_{H^0\tilde{\chi}_k^+\tilde{\chi}_k^+}^s) - \left[\frac{e^2 Q_b^2}{8\pi^2} \sum_{k=1,2} \bar{C}_{24}^{4,k} \cdot \right. \\
&\quad (A_h V_{h^0tt} V_{h^0\tilde{b}_k\tilde{b}_k} + A_H V_{H^0tt} V_{H^0\tilde{b}_k\tilde{b}_k}) + (Q_b, \tilde{b}, C^{4,k} \rightarrow Q_t, \tilde{t}, C^{5,k}) \Big]
\end{aligned}$$

$$\begin{aligned}
f_7^{tr,\hat{t}} &= f_8^{tr,\hat{t}} = f_9^{tr,\hat{t}} = f_{10}^{tr,\hat{t}} = -\frac{e^2}{4\pi^2} \sum_{k=1,2} m_{\tilde{\chi}_k^+} (C_0^{3,k} + 4C_{22}^{3,k} - 4C_{23}^{3,k}) \cdot \\
&\quad (A_h V_{h^0tt} V_{h^0\tilde{\chi}_k^+\tilde{\chi}_k^+}^s + A_H V_{H^0tt} V_{H^0\tilde{\chi}_k^+\tilde{\chi}_k^+}^s) - \left[\frac{e^2 Q_b^2}{4\pi^2} \sum_{k=1,2} (C_{23}^{4,k} - C_{22}^{4,k}) \cdot \right. \\
&\quad (A_h V_{h^0tt} V_{h^0\tilde{b}_k\tilde{b}_k} + A_H V_{H^0tt} V_{H^0\tilde{b}_k\tilde{b}_k}) + (Q_b, \tilde{b}, C^{4,k} \rightarrow Q_t, \tilde{t}, C^{5,k}) \Big]
\end{aligned}$$

$$f_{21}^{tr,\hat{t}} = f_{22}^{tr,\hat{t}} = \frac{-ie^2}{4\pi^2} \sum_{k=1,2} m_{\tilde{\chi}_k^+} C_0^{3,k} (A_A V_{A^0tt} V_{A^0\tilde{\chi}_k^+\tilde{\chi}_k^+}^{ps} + A_G V_{G^0tt} V_{G^0\tilde{\chi}_k^+\tilde{\chi}_k^+}^{ps})$$

$$f_i^{tr,\hat{t}} = 0, \quad (i = 3 \sim 6, 11 \sim 20),$$

where $\bar{C}_{24}^{3,k} = C_{24}^{3,k} - \frac{\Delta}{4}$ and $\bar{C}_{24}^{4,k} = C_{24}^{4,k} - \frac{\Delta}{4}$. The form factors in renormalized amplitude of the self-energy corrections $\mathcal{M}^{s,\hat{t}}$ from Fig.1(f) in t-channel, are expressed as:

$$f_i^{s,\hat{t}} = 0, \quad (i = 2 \sim 4, 6 \sim 10, 12 \sim 22),$$

$$\begin{aligned} f_1^{s,\hat{t}} &= \frac{-ie^2 Q_t^2 A_t^2}{16\pi^2} p_1 \cdot p_3 \left\{ 16\pi^2 (C_S^- + C_S^+ - m_t C_L - m_t C_R) \right. \\ &\quad + \sum_{i=1,4} \sum_{j=1,2} \left[m_{\tilde{\chi}_i^0} G_2^{t\tilde{t}_j \tilde{\chi}_i^0} \bar{B}_0^{3,i,j} - m_t G_1^{t\tilde{t}_j \tilde{\chi}_i^0} \bar{B}_1^{3,i,j} \right] \\ &\quad \left. + \sum_{i=1,2} \sum_{j=1,2} \left[m_{\tilde{\chi}_i^+} F_2^{t\tilde{b}_j \tilde{\chi}_i^+} \bar{B}_0^{4,i,j} - m_t F_1^{t\tilde{b}_j \tilde{\chi}_i^+} \bar{B}_1^{4,i,j} \right] \right\} \end{aligned}$$

$$\begin{aligned} f_{11}^{s,\hat{t}} &= \frac{f_5^{s,\hat{t}}}{2} = \frac{ie^2 Q_t^2 A_t^2}{16\pi^2} \left\{ 16\pi^2 \left[m_t (C_S^- + C_S^+) + (p_1 \cdot p_3 - m_t^2) (C_L + C_R) \right] \right. \\ &\quad + \sum_{i=1,4} \sum_{j=1,2} \left[m_t m_{\tilde{\chi}_i^0} G_2^{t\tilde{t}_j \tilde{\chi}_i^0} \bar{B}_0^{3,i,j} + (p_1 \cdot p_3 - m_t^2) G_1^{t\tilde{t}_j \tilde{\chi}_i^0} \bar{B}_1^{3,i,j} \right] \\ &\quad \left. + \sum_{i=1,2} \sum_{j=1,2} \left[m_t m_{\tilde{\chi}_i^+} F_2^{t\tilde{b}_j \tilde{\chi}_i^+} \bar{B}_0^{4,i,j} + (p_1 \cdot p_3 - m_t^2) F_1^{t\tilde{b}_j \tilde{\chi}_i^+} \bar{B}_1^{4,i,j} \right] \right\} \end{aligned}$$

In this work we adopted the definitions of two-, three-, four-point one-loop Passarino-Veltman integral functions as shown in reference[24] and all the vector and tensor integrals can be deduced in the forms of scalar integrals [25].

References

- [1] F. Abe et al., CDF Collaboration, Phys. Rev. Lett. 74, 2626(1995); S. Abachi et al., D0 Collaboration, Phys. Rev. Lett. 74, 2632(1995).
- [2] C. Caso, G. Conforto et al., 'Review of Particle Physics', Euro. Phys. J. bf C3, (1998)1; F. Abe et al., CDF Collaboration, Phys. Rev. Lett. 80, 2779(1998);

F. Abe et al., CDF Collaboration, Phys. Rev. Lett. 80, 2767(1998); S. Abachi et al., The D0 Collaboration, Phys. Rev. Lett. 79, 1197(1997).

- [3] H.E. Haber and G. Kane, Phys. Rep. 117(1985)75; J.Gunion and H.E. Haber, Nucl. Phys. **B272**, (1986)1.
- [4] C.S. Li et.al., Phys. Lett. **B379**, 135(1996); C.S. Li, et.al. Phys. Rev. **D52** 5014(1995)(Erratum: Phys. Rev. **D53** 4112(E) (1996)); S. Alam, et.al. Phys. Rev. **D55** 1307(1997); H.Y. Zhou, et.al. Phys. Rev. **D55** 4421(1997); J. Kim, et.al., Phys. Rev. **D54** 4364(1996).
- [5] W. Hollik and C. Schappacher, Nucl. Phys. **B545**, (1999)98-140.
- [6] I.F. Ginzbyrg, G.L. Kotkin, V.G. Serbo and V.I. Telnov, Pis'ma ZHETF 34 (1981)514; Nucl. Instr. Methods 205 (1983)47.
- [7] W.G. Ma, C.S. Li and L. Han, Phys. Rev. **D53** (1996)1304; V. Barger and R.J.N. Phillips, Phys. Rev. **D39** (1989)3310; A.C. Bawa et al, Z. Phys. C47, 75(1990); L. Han, C.G. Hu, C.S. Li and W.G. Ma, Phys. Rev. **D54** (1996)2363.
- [8] O.J.P. Eboli et al.,Phys. Rev. **D47** (1993)1889.
- [9] L. Han, W.G. Ma and Z.H. Yu, Phys. Rev. **D56** (1997)265; B. Kamal, Z. Merebashvili and A.P. Contogouris, Phys. Rev. **D51** (1995)4808.
- [10] A. Denner, S. Dittmaier and M. Strobel, Phys. Rev. **D53** (1996)44.
- [11] C.S. Li, J.M. Yang, Y.L. Zhou and H.Y. Zhou, Phys. Rev. **D54** (1996)4662.
- [12] M.L. Zhou, W.G. Ma, L. Han, Y. Jiang and H. Zhou, J. of Phys. G25, 27(1999).
- [13] J. Ellis and S. Rudaz, Phys. Lett. **B128**, 248(1983);
- [14] I.F. Ginzburg, G.L. Kotkin, V.G. Serbo and V.I. Telnov, Pis'ma ZHETF 34(1981)514; Nucl. Instr. Methods 205 (1983)47.
- [15] R.Brankenbecler and S.D.Drell, Phys. Rev. Lett. 61 (2324)1988; F.Halzen, C.S.Kim and M.L.Stong, Phys. Lett. B274, (489)1992; M.Drees and R.M.Godbole, Phys. Lett. 67 (1991)1189.

- [16] V.Telnov, Nucl. Instr. Methods A294, (72)1990.
- [17] M.Carena, M. Quiros and C.E.M. Wagner, Phys. Lett **B355**, (1995)209.
- [18] see for examples, J.R. Espinosa, and M Quiros, Phys. Lett **B266** (1991)389; K. Gunion and A. Turski, Phys. Rev. **D39** (1989)2701 and **D40** (1990)2333; M.Carena, M. Quiros and C.E.M. Wagner, Nucl. Phys.**B461**, (1996)407.
- [19] D.M. Copper, D.R.T. Jones and P.van Nieuwenhuizen, Nucl. Phys. **B167**(1980) 479; W. Siegel, Phys. Lett. **B84**, (1979)193.
- [20] D.A. Ross and J.C. Taylor, Nucl. Phys. **B51**, (1979)25.
- [21] A. Goto and T. Kon, Europhys. Lett. 13,(1990)211; 14 (1991)75; F. Cuypart, G.J. Oldenborgh and R. Ruckl, Nucl. Phys.**B409**, (1993)144; M. Hoike, T. Nonaka and T. Kon, Phys. Lett. **B357** (1995)232.
- [22] Bernd A. Kniehl and A. Pilaftsis, Nucl. Phys. B474, (1996)286.
- [23] M.L. Zhou, W.G. Ma, L. Han, Y. Jiang and H. Zhou, 'One-loop quark and squark corrections to the lightest chargino pair production in photon-photon collisions', hep-ph/9903376, to be appeared in J. of Phys G.
- [24] Bernd A. Kniehl, Phys. Rep. 240 (1994)211.
- [25] G. Passarino and M. Veltman, Nucl. Phys. **B160**, 151(1979).

Figure captions

Fig.1 The Feynman diagrams at tree level and EW-like one-loop diagrams in the MSSM for subprocess $\gamma\gamma \rightarrow t\bar{t}$. (a) tree level diagram; (b) vertex diagrams; (c) box diagrams; (d) quartic coupling diagram; (e) triangle diagrams, and (f) self-energy diagrams. The \tilde{t} and \tilde{b} that appear in diagrams have two physical particle eigenstates, while $\tilde{\chi}^0$ have four mass eigenstates, and $\tilde{\chi}^+$ have two. The diagrams with exchanging incoming photons are not shown in the figures except for Fig.1(d).

Fig.2 The corrections as the functions of c.m.s. energy $\sqrt{\hat{s}}$ for subprocess $\gamma\gamma \rightarrow t\bar{t}$. (a) the absolute corrections; (b) the relative corrections. The solid line is for $\tan\beta = 4$ and the dashed line is for $\tan\beta = 40$.

Fig.3 The relative corrections as the functions of M_Q for subprocess $\gamma\gamma \rightarrow t\bar{t}$. The solid line is for $\tan\beta = 4$, $\sqrt{\hat{s}} = 500 \text{ GeV}$, the dashed line is for $\tan\beta = 40$, $\sqrt{\hat{s}} = 500 \text{ GeV}$, the dotted line is for $\tan\beta = 4$, $\sqrt{\hat{s}} = 1 \text{ TeV}$, and the dash-dotted line is for $\tan\beta = 40$, $\sqrt{\hat{s}} = 1 \text{ TeV}$.

Fig.4 The relative corrections as the functions of $M_{SU(2)}$ for subprocess $\gamma\gamma \rightarrow t\bar{t}$. The solid line is for $\tan\beta = 4$, $\sqrt{\hat{s}} = 500 \text{ GeV}$, the dashed line is for $\tan\beta = 40$, $\sqrt{\hat{s}} = 500 \text{ GeV}$, the dotted line is for $\tan\beta = 4$, $\sqrt{\hat{s}} = 1 \text{ TeV}$, and the dash-dotted line is for $\tan\beta = 40$, $\sqrt{\hat{s}} = 1 \text{ TeV}$.

Fig.5 The relative corrections as the functions of μ for subprocess $\gamma\gamma \rightarrow t\bar{t}$. The solid line is for $\tan\beta = 4$, $\sqrt{\hat{s}} = 500 \text{ GeV}$, the dashed line is for $\tan\beta = 40$, $\sqrt{\hat{s}} = 500 \text{ GeV}$, the dotted line is for $\tan\beta = 4$, $\sqrt{\hat{s}} = 1 \text{ TeV}$, and the dash-dotted line is for $\tan\beta = 40$, $\sqrt{\hat{s}} = 1 \text{ TeV}$.

Fig.6 The cross section including the contributions of one-loop EW-like corrections for the parent process as the function of e^+e^- energy \sqrt{s} .

Fig.7 The relative correction for the parent process as the function of e^+e^- energy \sqrt{s} . The solid line is for $\tan\beta = 4$ and the dashed line is for $\tan\beta = 40$.

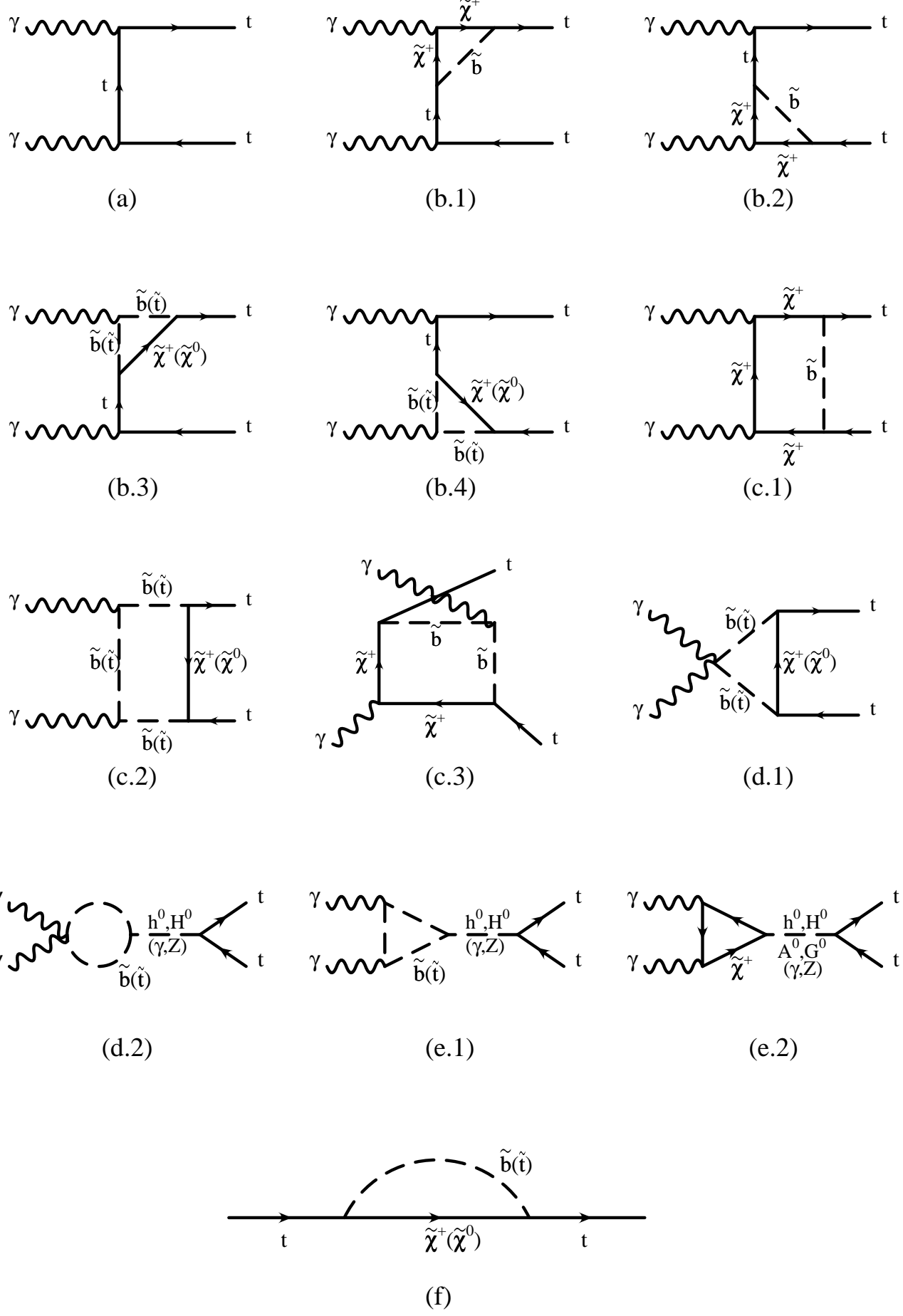


Fig.1

Fig.2(a)

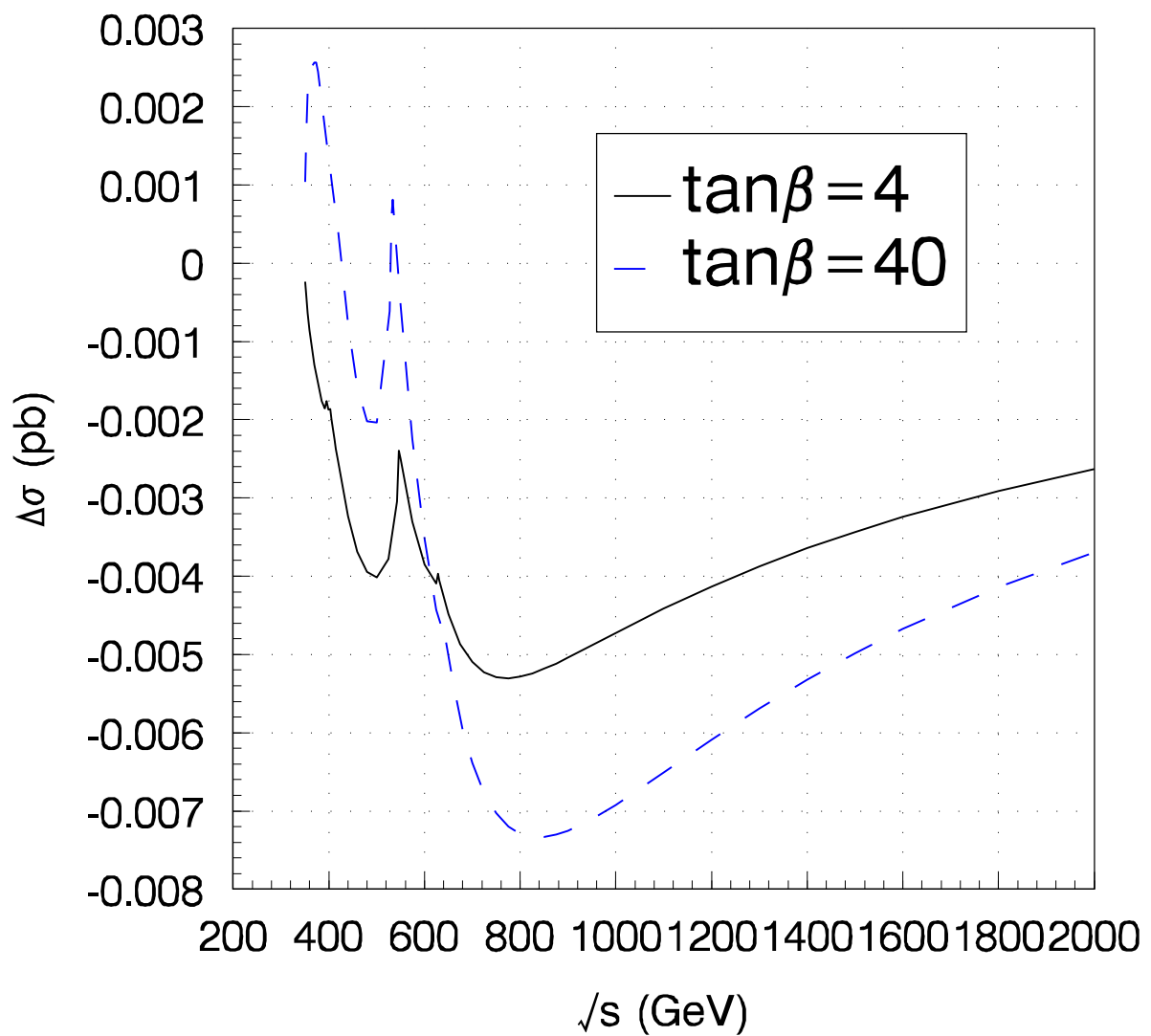


Fig.2(b)

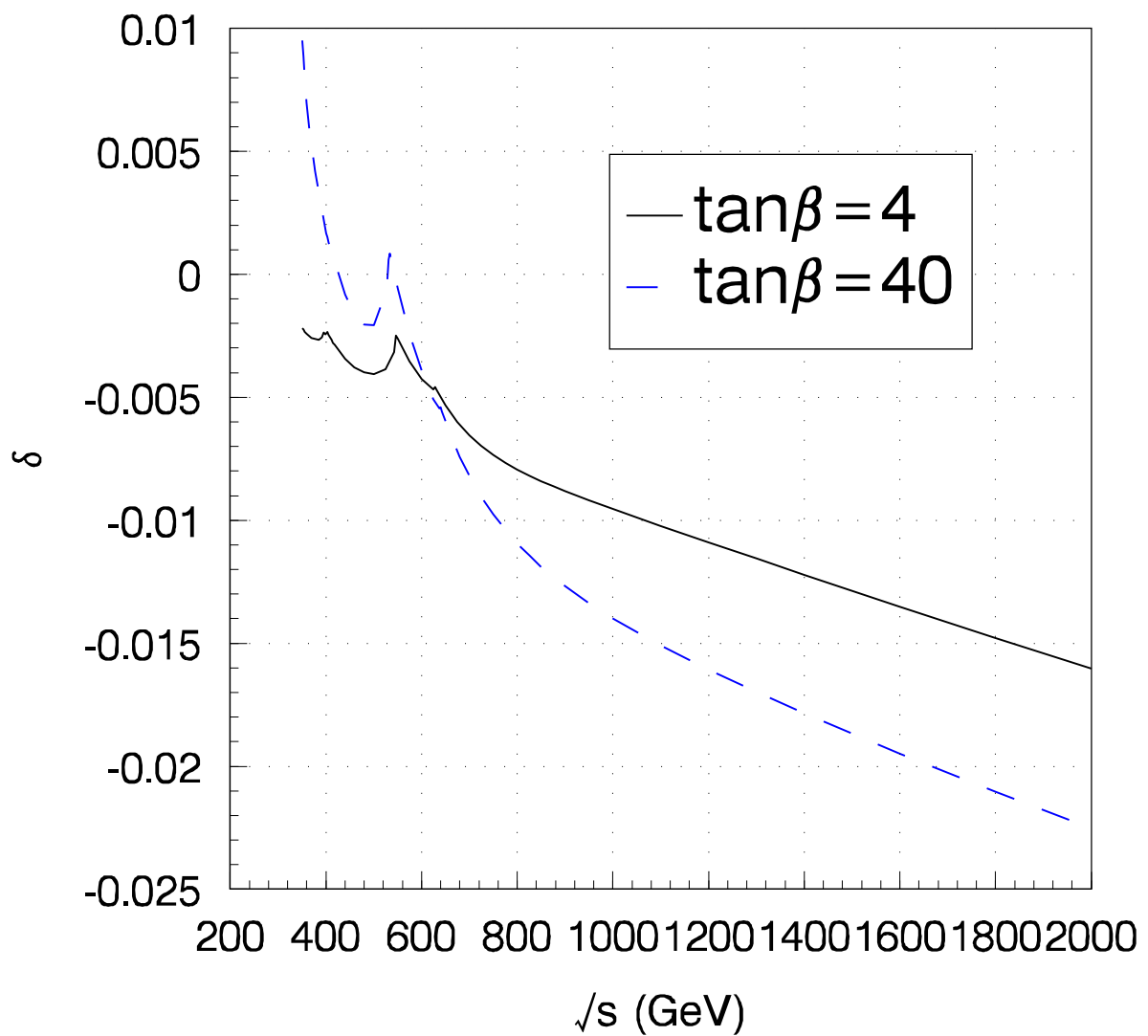


Fig.3

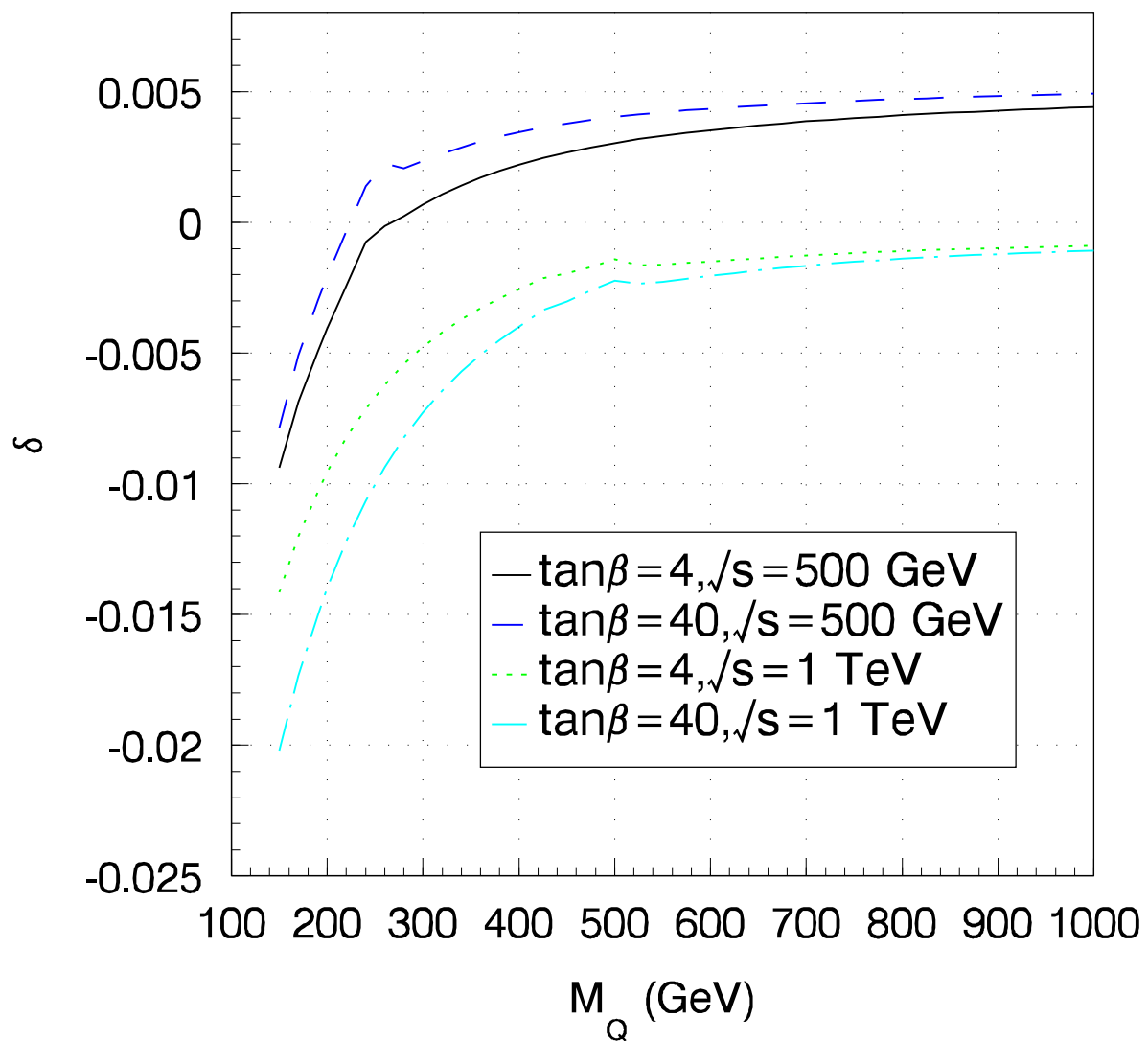


Fig.4

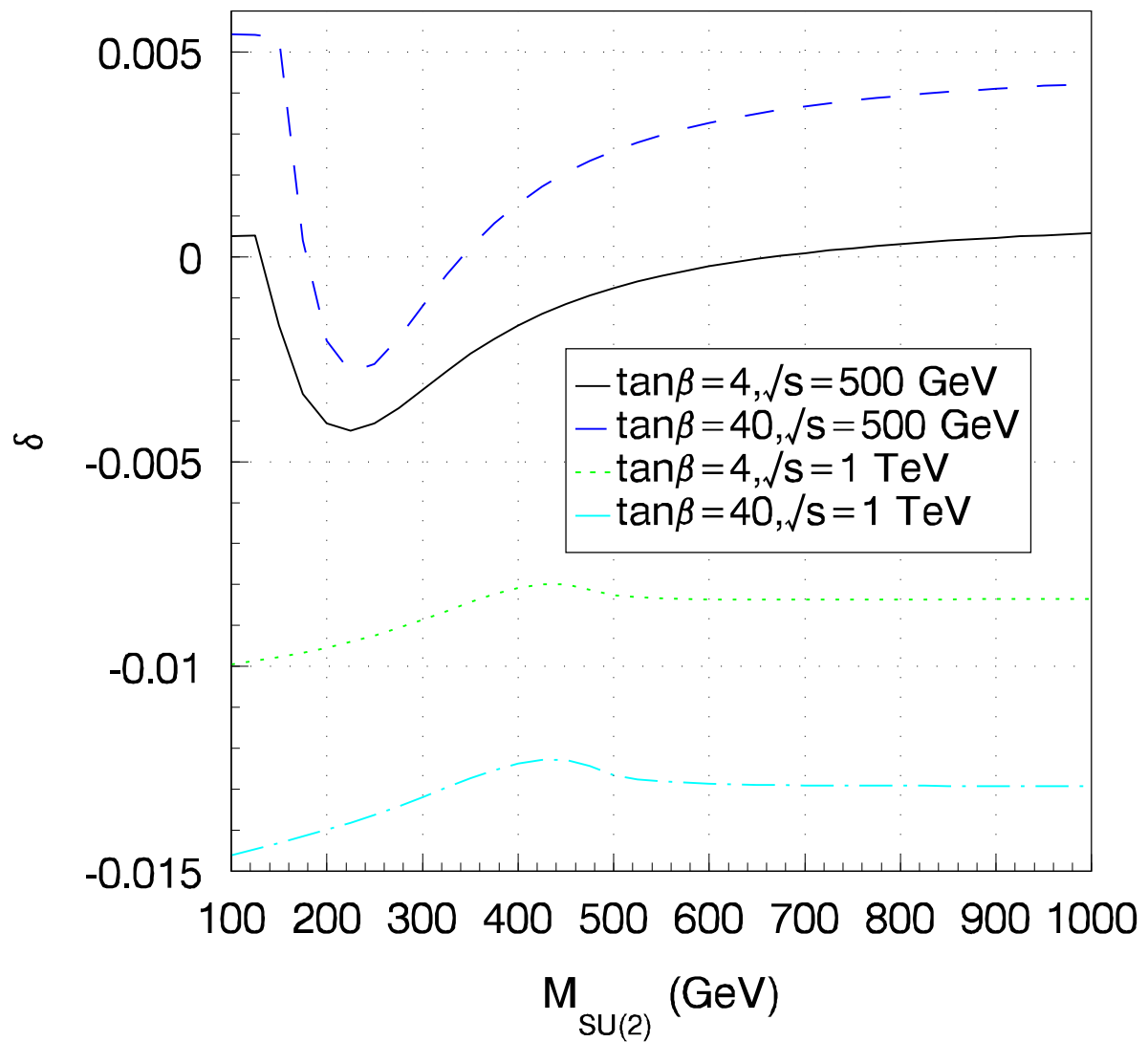


Fig.5

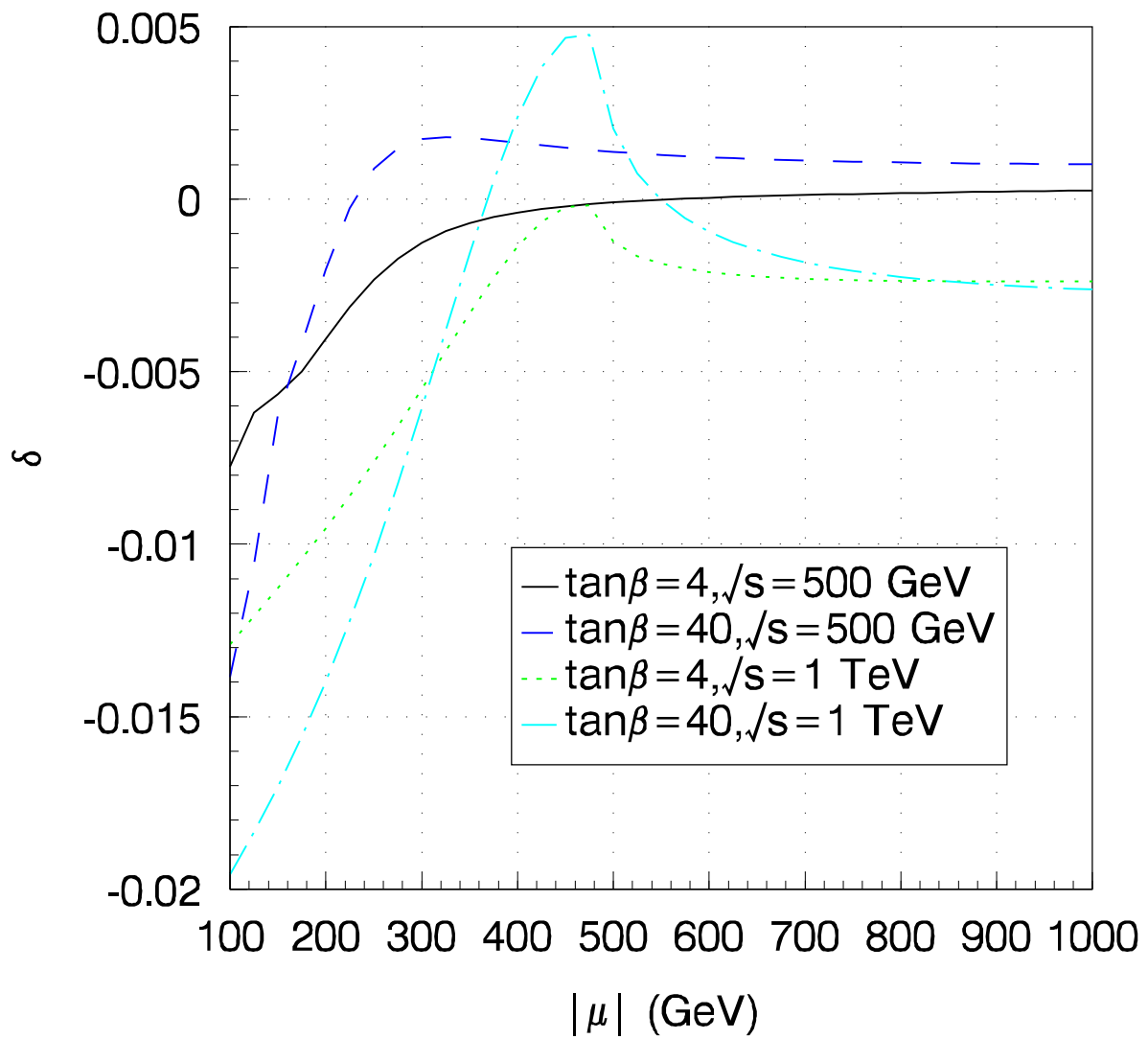


Fig.6

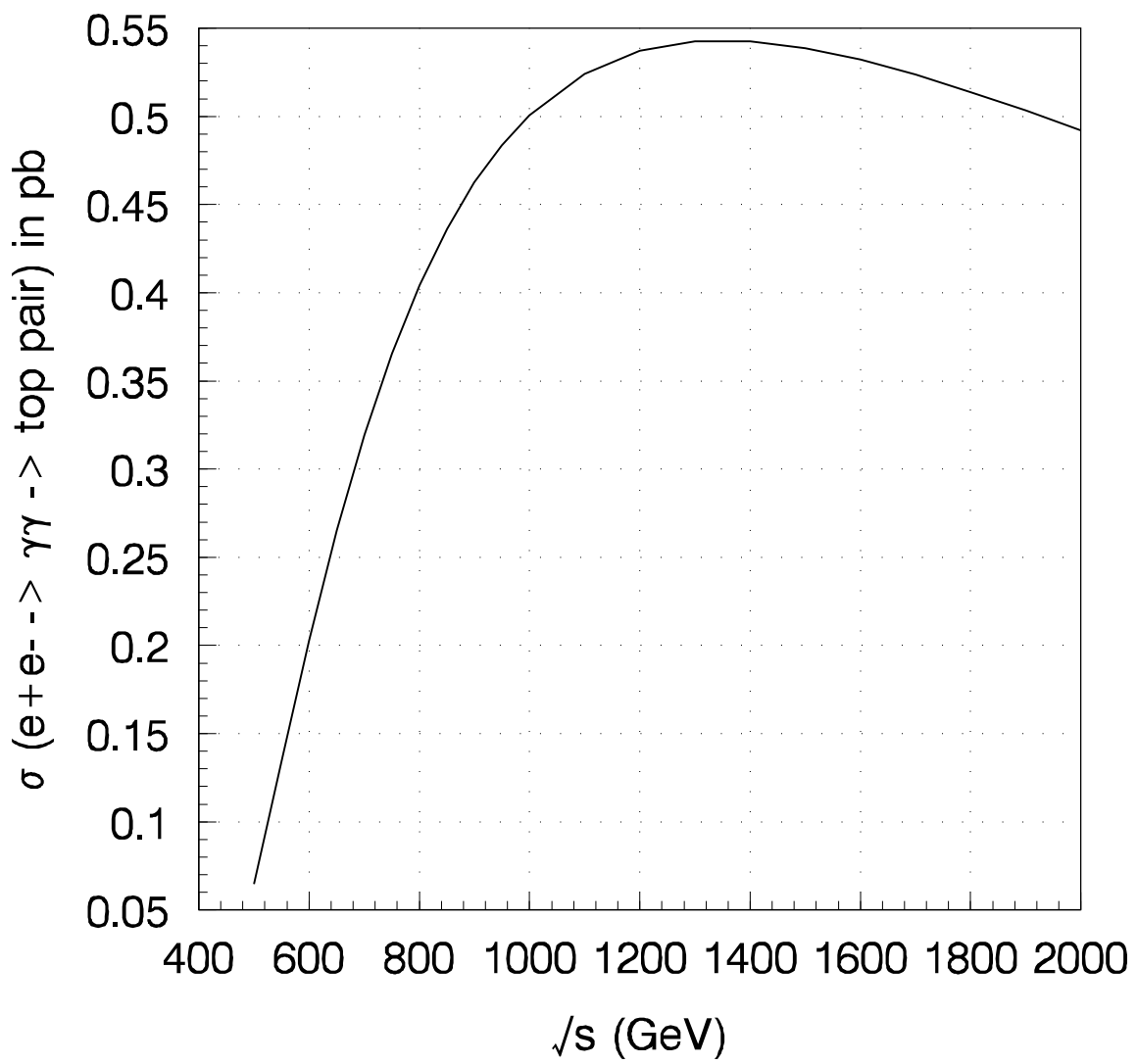


Fig.7

